

Review Article

Diffractive Bremsstrahlung in Hadronic Collisions

Roman Pasechnik,¹ Boris Kopeliovich,² and Irina Potashnikova²

¹Department of Astronomy and Theoretical Physics, Lund University, 223-62 Lund, Sweden

²Departamento de Física and Centro Científico Tecnológico de Valparaíso, Universidad Técnica Federico Santa María, Casilla 110-V, Avenida España 1680, 239-0123 Valparaíso, Chile

Correspondence should be addressed to Roman Pasechnik; roman.pasechnik@thep.lu.se

Received 6 April 2015; Revised 9 July 2015; Accepted 12 July 2015

Academic Editor: Sally Seidel

Copyright © 2015 Roman Pasechnik et al. This is an open access article distributed under the Creative Commons Attribution License, which permits unrestricted use, distribution, and reproduction in any medium, provided the original work is properly cited. The publication of this article was funded by SCOAP³.

Production of heavy photons (Drell-Yan), gauge bosons, Higgs bosons, and heavy flavors, which is treated within the QCD parton model as a result of hard parton-parton collision, can be considered a bremsstrahlung process in the target rest frame. In this review, we discuss the basic features of the diffractive channels of these processes in the framework of color dipole approach. The main observation is a dramatic breakdown of diffractive QCD factorisation due to the interplay between soft and hard interactions, which dominates these processes. This observation is crucial for phenomenological studies of diffractive reactions in high energy hadronic collisions.

1. Introduction

Diffractive production of particles in hadron-hadron scattering at high energies is one of the basic tools, experimental and theoretical, giving access to small x and nonperturbative QCD physics. The characteristic feature of diffractive processes at high energies is the presence of a large rapidity gap between the remnants of the beam and target.

The understanding of the mechanisms of inelastic diffraction came with the pioneering works of Glauber [1], Feinberg and Pomerenchuk [2], and Good and Walker [3]. Here diffraction is conventionally viewed as a shadow of inelastic processes. If the incoming plane wave contains components interacting differently with the target, the outgoing wave will have a different composition; that is, besides elastic scattering a new *diffractive* state will be created resulting in a new combination of the Fock components (for a detailed review on QCD diffraction, see [4, 5]). Diffraction, which is usually a soft process, is difficult to predict from the first principles, because it involves poorly known nonperturbative effects. Therefore, diffractive reactions characterized by a hard scale deserve a special attention. It is tempting, on analogy to inclusive reactions, to expect that QCD factorization holds for such diffractive processes. Although factorization of short

and long distances still holds in diffractive DIS, the fracture functions are not universal and cannot be used for other diffractive processes.

Examples of breakdown of diffractive factorization are the processes of production of Drell-Yan dileptons [6, 7], gauge bosons [8], and heavy flavors [9]. Factorization turns out to be broken in all these channels in spite of presence of a hard scale given by the large masses of produced particles; it occurs due to the interplay of short- and long-range interactions.

The main difficulty in formulation of a theoretical QCD-based framework for diffractive scattering is caused by the essential contamination of soft, nonperturbative interactions. For example, diffractive deep-inelastic scattering (DIS), $\gamma^* p \rightarrow \bar{q}q p$, although it is a higher twist process, is dominated by soft interactions [10]. Within the dipole approach [11] such a process looks like a linear combination of elastic scattering amplitudes for $\bar{q}q$ dipoles of different sizes. Although formally the process $\gamma^* \rightarrow \bar{q}q$ is an off-diagonal diffraction, it does not vanish in the limit of unitarity saturation, the so-called black-disc limit. This happens because the initial and final $\bar{q}q$ distribution functions are not orthogonal. Similar features exhibit the contribution of higher Fock components of the photon, for example, the leading twist diffraction $\gamma^* \rightarrow \bar{q}qg$.

Diffractive excitation of the beam hadron has been traditionally used as a way to measure the Pomeron-hadron total cross section [4]. This idea, extended to DIS, allows measuring the structure function of the Pomeron [12]. The next step, which might look natural, is to assume that QCD factorization holds for diffraction and to employ the extracted parton distributions in the Pomeron in order to predict the hard diffraction cross sections in hadronic collisions. However, such predictions for hard hadronic diffraction, for example, high- p_T dijet production, failed by an order of magnitude [13, 14]. In this case the situation is different and more complicated; namely, factorization of small and large distances in hadronic diffraction is broken because of presence of spectator partons and due to large hadronic sizes.

The cross section of diffractive production of W boson in $p\bar{p}$ collisions, measured by the CDF experiment [15, 16], was also found to be six times smaller than what was predicted relying on factorization and diffractive DIS data [17]. Besides, the phenomenological models based on diffractive factorization, which are widely discussed in the literature (see, e.g., [18, 19]), predict a significant increase of the ratio of the diffractive-to-inclusive gauge bosons production cross sections with energy. The diffractive QCD factorization in hadron collisions is, however, severely broken by the interplay of hard and soft dynamics, as was recently advocated in [7, 8], and this review is devoted to study of these important effects within the color dipole phenomenology.

The processes under discussion—single diffractive Drell-Yan [6, 7], diffractive radiation of vector (Z, W^\pm) bosons [8], diffractive heavy flavor production [9], and diffractive associated heavy flavor and Higgs boson production [20]—correspond to off-diagonal diffraction. While diagonal diffraction is enhanced by absorption effects (in fact it is a result of absorption), the off-diagonal diffractive processes are suppressed by absorption and even vanish in the limit of maximal absorption, that is, in the black-disc limit.

The absorptive corrections, also known as the survival probability of rapidity gaps [21], are related to initial- and final-state interactions. Usually the survival probability is introduced into the diffractive cross section in a probabilistic way [22] and is estimated in simplified models such as eikonal, quasi-eikonal, and two-channel approximations.

According to the Good-Walker basic mechanism of diffraction, the off-diagonal diffractive amplitude is a linear combination of diagonal (elastic) diffractive amplitudes of different Fock components in the projectile hadron. Thus, the absorptive corrections naturally emerge at the amplitude level as a result of mutual cancellations between different elastic amplitudes. Therefore, there is no need to introduce any additional multiplicative gap survival probability factors. Within the light-cone color dipole approach [11] a diffractive process is considered a result of elastic scattering of $\bar{q}q$ dipoles of different sizes emerging in incident Fock states. The study of the diffractive Drell-Yan reaction performed in [6] has revealed importance of soft interactions with the partons spectators, which contribute on the same footing as hard perturbative ones and strongly violate QCD factorization.

One of the advantages of the dipole description is the possibility to calculate directly (although in a process-dependent

way) the full diffractive amplitude, which contains all the absorption corrections by employing the phenomenological universal dipole cross section (or dipole elastic amplitudes) fitted to DIS data. The gap survival amplitude can be explicitly singled out as a factor from the diffractive amplitude being a superposition of dipole scatterings at different transverse separations.

Interestingly, besides interaction with the spectator projectile partons, there is another important source for diffractive factorization breaking. Even a single quark, having no spectator comovers, cannot radiate Abelian fields (γ, Z, W^\pm, H) interacting diffractively with the target with zero-transverse-momentum transfer [23], that is, in forward direction scattering. This certainly contradicts the expectations based on diffractive factorization. In the case of a hadron beam the forward directions for the hadron and quark do not coincide, so a forward radiation is possible but is strongly suppressed (see below).

Interaction with the spectator partons opens new possibilities for diffractive radiation in forward direction; namely, the transverse momenta transferred to different partons can compensate each other. It was found in [6–8] that this contribution dominates the forward diffractive Abelian radiation cross section. This mechanism leads to a dramatic violation of diffractive QCD factorization, which predicts diffraction to be a higher twist effect, while it turns out to be a leading twist effect due to the interplay between the soft and hard interactions. Although diffractive gluon radiation off a forward quark does not vanish due to possibility of glue-gluon interaction, the diffractive factorization breaking in non-Abelian radiation is still important.

In this review, we briefly discuss the corresponding effects whereas more details can be found in [6–9, 20].

2. Color Dipole Picture of Diffractive Excitation

Single diffractive scattering and production of a new (diffractive) state, that is, diffractive excitation, emerge as a consequence of quantum fluctuations in projectile hadron. The orthogonal hadron state $|h\rangle$ can be excited due to interactions but can be decomposed over the orthogonal and complete set of eigenstates of interactions $|\alpha\rangle$ as [11, 24, 25]

$$|h\rangle = \sum C_\alpha^h |\alpha\rangle, \quad (1)$$

$$\hat{f}_{\text{el}} |\alpha\rangle = f_\alpha |\alpha\rangle,$$

where \hat{f}_{el} is the elastic amplitude operator and f_α is one of its eigenstates. The eigenamplitudes f_α are the same for different types of hadrons. Hence, the elastic $h \rightarrow h$ and single diffractive $h \rightarrow h'$ amplitudes can be conveniently written in terms of the elastic eigenamplitudes f_α and coefficients C_α^h ; that is,

$$f_{\text{el}}^{hh} = \sum |C_\alpha^h|^2 f_\alpha, \quad (2)$$

$$f_{\text{sd}}^{hh'} = \sum (C_\alpha^{h'})^* C_\alpha^h f_\alpha,$$

respectively, such that the forward single diffractive cross section

$$\sum_{h' \neq h} \left. \frac{d\sigma_{sd}}{dt} \right|_{t=0} = \frac{1}{4\pi} \left[\sum_{h'} |f_{sd}^{hh'}|^2 - |f_{el}^{hh}|^2 \right] \quad (3)$$

$$= \frac{\langle f_\alpha^2 \rangle - \langle f_\alpha \rangle^2}{4\pi}$$

is given by the dispersion of the eigenvalues distribution.

It was suggested in [11] that eigenstates of QCD interactions are color dipoles, such that any diffractive amplitude can be considered a superposition of universal elastic dipole amplitudes. Such dipoles experience only elastic scattering and are characterized only by transverse separation \vec{r} . The total hadron-proton cross section is then given by its eigenvalue, the universal dipole cross section

$$\sigma(\vec{r}) \equiv \int d^2b 2 \text{Im} f_{el}(\vec{b}, \vec{r}), \quad (4)$$

as follows:

$$\sigma_{tot}^{hp} = \sum |C_\alpha^h|^2 \sigma_\alpha = \int d^2r |\Psi_h(\vec{r})|^2 \sigma(\vec{r}) \equiv \langle \sigma(\vec{r}) \rangle, \quad (5)$$

where $\Psi_h(\vec{r})$ is the ‘‘hadron-to-dipole’’ transition wave function (incident parton momentum fractions are omitted). The dipole description of diffraction is based on the fact that dipoles of different transverse size r_\perp interact with different cross sections $\sigma(r_\perp)$, leading to the single inelastic diffractive scattering with a cross section, which in the forward limit is given by [11]

$$\left. \frac{\sigma_{sd}}{dp_\perp^2} \right|_{p_\perp=0} = \frac{\langle \sigma^2(\vec{r}) \rangle - \langle \sigma(\vec{r}) \rangle^2}{16\pi}, \quad (6)$$

where p_\perp is the transverse momentum of the recoil proton, $\sigma(r)$ is the universal dipole-proton cross section, and operation $\langle \dots \rangle$ means averaging over the dipole separation. For low and moderate energies, $\sigma(r)$ also depends on Bjorken variable x whereas, in the high energy limit, the collision c.m. energy squared s is a more appropriate variable [23, 26]. The phenomenological dipole cross section fitted to data on inclusive DIS implicitly incorporates the effect of gluon bremsstrahlung. The latter is more important on a hard scale; this is why the small-distance dipole cross section rises faster with $1/x$.

Even for the simplest quark-antiquark dipole configuration, a theoretical prediction of the partial dipole amplitude $f_{el}^{q\bar{q}}(\vec{b}, \vec{r})$ and the dipole cross section $\sigma_{q\bar{q}}(\vec{r})$ from the first QCD principles is still a big challenge so these are rather fitted to data. The universality of the dipole scattering, however, enables us to fit known parameterizations to one set of known data (e.g., inclusive DIS) and use them for accurate predictions of other yet unknown observables (e.g., rapidity gap processes).

Indeed, at small Bjorken x in DIS the virtual photon exhibits partonic structure as shown in Figure 1. The leading

order configuration, the $q\bar{q}$ dipole, then elastically rescatters off the proton target p providing a phenomenological access to $\sigma_{q\bar{q}}(\vec{r}, x)$. When it comes to diffractive DIS schematically represented in Figure 2, the corresponding single diffractive cross section in the forward proton limit $t \rightarrow 0$ is given by the dipole cross section squared; that is,

$$16\pi \left. \frac{d\sigma_{sd}^{Y^*p}(x, Q^2)}{dt} \right|_{t=0} \quad (7)$$

$$= \int d^2r \int_0^1 d\alpha |\Psi_{Y^*}(\vec{r}, \alpha, Q^2)| \sigma_{q\bar{q}}^2(\vec{r}, x),$$

where α is the light-cone momentum fraction of the virtual photon carried by the quark. Here, the dipole size \vec{r} is regulated by the photon light-cone wave function Ψ_{Y^*} , which can be found, for example, in [29]. The mean dipole size squared is inversely proportional to the quark energy squared:

$$\langle r^2 \rangle \sim \frac{1}{\epsilon^2} = \frac{1}{Q^2 \alpha (1 - \alpha) + m_q^2}. \quad (8)$$

The dipole size is assumed to be preserved during scattering in the high energy limit.

Hard and soft hadronic fluctuations have small $\langle r^2 \rangle \sim 1/Q^2$ (nearly symmetric $\alpha \gg m_q^2/Q^2$ configuration) and large $\langle r^2 \rangle \sim 1/m_q^2$, $m_q \sim \Lambda_{\text{QCD}}$ (aligned jet $\alpha \sim m_q^2/Q^2$ configuration) sizes, respectively. Remarkably enough, soft fluctuations play a dominant role in diffractive DIS in variance with inclusive DIS [10]. Although such soft fluctuations are very rare, their interactions with the target occur with a large cross section $\sigma \sim 1/m_q^2$ which largely compensate their small $\sim m_q^2/Q^2$ weights. On the other hand, abundant hard fluctuations with nearly symmetric small-size dipoles $\langle r^2 \rangle \sim 1/Q^2$ have vanishing (as $1/Q^2$) cross section. It turns out that, in inclusive DIS, both hard and soft contributions to the total cross section behave as $1/Q^2$ (semihard and semisoft), while in diffractive DIS the soft fluctuations $\sim 1/m_q^2 Q^2$ dominate over the hard ones $\sim 1/Q^4$. This also explains why the ratio σ_{sd}/σ_{inc} in DIS is nearly Q^2 independent as well as a higher twist nature of the diffractive DIS.

The main ingredient of the dipole approach is the phenomenological dipole cross section, which is parameterized in the saturated form [26],

$$\sigma_{q\bar{q}}(r, x) = \sigma_0 \left(1 - e^{-r_p^2/R_0^2(x)} \right), \quad (9)$$

and fitted to DIS data. Here, x is the Bjorken variable, $\sigma_0 = 23.03$ mb, and $R_0(x) = 0.4 \text{ fm} \times (x/x_0)^{0.144}$ and $x_0 = 0.003$. In pp collisions x is identified with gluon $x_2 = M^2/x_1 s \ll 1$, where M is the invariant mass of the produced system and s is the pp c.m. energy. This parametrization, though oversimplified (compare with [30]), is rather successful in description of experimental HERA data with a reasonable accuracy.

In soft processes, however, the Bjorken variable x makes no sense, and gluon-target collision c.m. energy squared

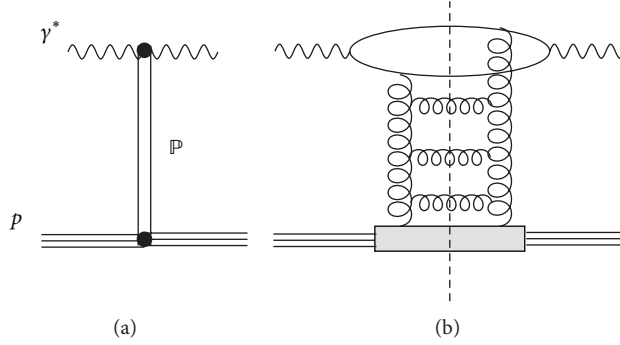


FIGURE 1: The DIS cross section via phenomenological Pomeron exchange (a) and a perturbative QCD ladder (b). At small x the virtual photon fluctuates into $q\bar{q}$ dipole and more complicated Fock states which then interact with the hadronic target.

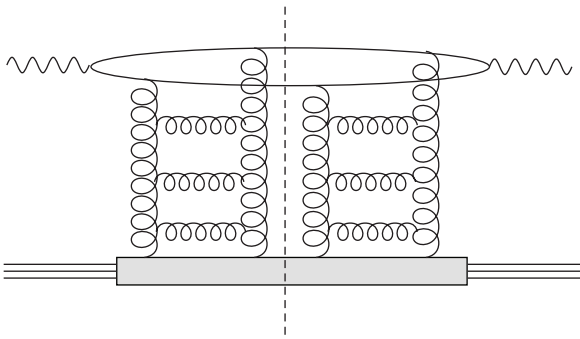


FIGURE 2: The diffractive DIS cross section via double ladder exchange.

$\hat{s} = x_1 s$ (s is the pp c.m. energy) is a more appropriate variable, while the saturated form (9) should be retained [23]. The corresponding parameterizations for $\sigma_0 = \sigma_0(\hat{s})$ and $R_0 = R_0(\hat{s})$ read as follows:

$$R_0(\hat{s}) = 0.88 \text{ fm} \left(\frac{s_0}{\hat{s}} \right)^{0.14}, \quad (10)$$

$$\sigma_0(\hat{s}) = \sigma_{\text{tot}}^{\pi p}(\hat{s}) \left(1 + \frac{3R_0^2(\hat{s})}{8 \langle r_{\text{ch}}^2 \rangle_{\pi}} \right),$$

where the pion-proton total cross section is parametrized as [31] $\sigma_{\text{tot}}^{\pi p}(\hat{s}) = 23.6(\hat{s}/s_0)^{0.08}$ mb, $s_0 = 1000 \text{ GeV}^2$; the mean pion radius squared is [32] $\langle r_{\text{ch}}^2 \rangle_{\pi} = 0.44 \text{ fm}^2$. An explicit analytic form of the x - and \hat{s} -dependent parameterizations for the elastic amplitude $f_{\text{el}}(\vec{b}, \vec{r})$ accounting for information about the dipole orientation with respect to the color background field (i.e., the angular dependence between \vec{r} and \vec{b}) can be found in [33–35].

Ansatz (9) incorporates such important phenomenon as saturation at a soft scale since it levels off at $r \gg R_0$. Another important feature is vanishing of the cross section at small $r \rightarrow 0$ as $\sigma_{q\bar{q}} \propto r^2$ [11]. This is a general property called color transparency which reflects the fact that a point-like colorless object does not interact with external color fields. Finally, the quadratic r -dependence is an immediate consequence of gauge invariance and nonabelianity of interactions in QCD.

3. Diffractive Abelian Radiation: Regge versus Dipole Approach

3.1. Diffractive Factorization. The cross section of the inclusive Drell-Yan (DY) is expressed via the dipole cross section in a way similar to DIS [36]:

$$\frac{d\sigma_{\text{DY}}(qp \rightarrow \gamma^* X)}{d\alpha dM^2} = \int d^2r |\Psi_{q\gamma^*}(\vec{r}, \alpha)|^2 \sigma_{q\bar{q}}(\alpha\vec{r}), \quad (11)$$

where α is the light-cone momentum fraction carried by the heavy photon off the parent quark. QCD factorization relates inclusive DIS with DY, and similarity between these processes is the source of universality of the hadron PDFs.

Now, consider the forward single diffractive Drell-Yan (DDY) and vector bosons production $G = Z, W^\pm$ in pp collisions which is characterized by a relatively small momentum transfer between the colliding protons. In particular, one of the protons, for example, p_1 , radiates a hard virtual gauge G^* boson with $k^2 = M^2 \gg m_p^2$ and hadronizes into a hadronic system X both moving in forward direction and separated by a large rapidity gap from the second proton p_2 , which remains intact. In the DDY case,

$$p_1 + p_2 \rightarrow X + (\text{gap}) + p_2, \quad (12)$$

$$X \equiv \gamma^* (l^+ l^-) + Y.$$

Both the dilepton and X , the debris of p_1 , stay in the forward fragmentation region. In this case, the virtual photon is predominantly emitted by the valence quarks of proton p_1 .

In some of the previous studies [18, 37] of the single diffractive Drell-Yan reaction the analysis was made within the phenomenological Pomeron-Pomeron and γ -Pomeron fusion mechanisms using the Ingelman-Schlein approach [12] based on diffractive factorization. In analogy to the proven collinear factorization [38] for inclusive processes, one assumes factorization of short and long distances in diffractive processes characterized by a hard scale. Besides one assumes that the soft part of the interaction is carried out by Pomeron exchange, which is universal for different diffractive processes; that is, Regge factorization is assumed as well. That could be true if the Pomeron were a true Regge pole, which is not supported by any known dynamical model.

The above two assumptions lead to the following form of the diffractive DY cross section [37, 39] expressed in terms of the Pomeron PDFs $F_{\bar{q}/\mathbb{P}}$:

$$\sigma_{\text{sd}}^{\text{DY}} = G_{\mathbb{P}/p} \otimes F_{\bar{q}/\mathbb{P}} \otimes F_{q/p} \otimes \hat{\sigma}(q\bar{q} \rightarrow \bar{l}l). \quad (13)$$

The diffractive factorization leads to specific features of the differential DY cross sections similar to those in diffractive DIS process, for example, a slow increase of the diffractive-to-inclusive DY cross sections ratio with c.m.s. energy \sqrt{s} , its practical independence on the hard scale, and the invariant mass of the lepton pair squared, M^2 [18].

However, presence of spectator partons in hadronic collisions leads to a dramatic breakdown of diffractive factorization of short and long distances. Contrary to inclusive processes, where spectator partons do not participate in the hard reactions in leading order, below we demonstrate that in diffraction the spectator partons do participate on a soft scale; that is, their contribution is enhanced by Q^2/Λ^2 . In particular, the spectator partons generate large absorptive corrections, usually called rapidity gap survival probability, which cause a strong suppression of the diffractive cross section compared with (13).

One can derive Regge behavior of the diffractive cross section of heavy photon production in terms of the usual light-cone variables:

$$\begin{aligned} x_1 &= \frac{p_\gamma^+}{p_1^+}, \\ x_2 &= \frac{p_\gamma^-}{p_2^-}, \end{aligned} \quad (14)$$

so that $x_1 x_2 = (M^2 + k_T^2)/s$ and $x_1 - x_2 = x_F$, where M , k_T , and x_F are the invariant mass, transverse momentum, and Feynman variable of the heavy photon (dilepton).

In the limit of small $x_1 \rightarrow 0$ and large $z_p \equiv p_4^+/p_2^+ \rightarrow 1$ the diffractive DY cross section is given by the Mueller graph shown in Figure 4. In this case, the end-point behavior is dictated by the following general result:

$$\left. \frac{d\sigma}{dz_p dx_1 dt} \right|_{t \rightarrow 0} \propto \frac{1}{(1 - z_p)^{2\alpha_{\mathbb{P}}(t)-1} x_1^\varepsilon}, \quad (15)$$

where $\alpha_{\mathbb{P}}(t)$ is the Pomeron trajectory corresponding to the t -channel exchange and ε is equal to 1 or 1/2 for the Pomeron \mathbb{P} or Reggeon \mathbb{R} exchange corresponding to γ^* emission from sea or valence quarks, respectively. Thus, the diffractive Abelian radiation process $pp \rightarrow (X \rightarrow G^* + Y)p$ at large Feynman $x_F \rightarrow 1$, or small

$$\xi = 1 - x_F = \frac{M_X^2}{s} \ll 1, \quad (16)$$

is described by triple-Regge graphs in Figure 5 where we also explicitly included radiation of a virtual gauge boson G^* . The Feynman graphs, corresponding to the corresponding triple-Regge terms, are shown in Figure 5 (second and third rows).

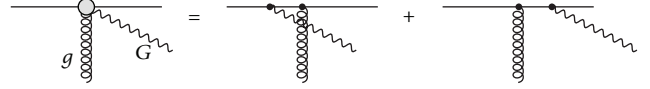


FIGURE 3: Gauge boson radiation by a projectile quark in the target rest frame.

The (ba) and (ca) diagrams illustrate the 3-Pomeron term; that is,

$$\frac{d\sigma_{\text{diff}}^{\text{PPP}}}{d\xi dt} \propto \xi^{-\alpha_{\mathbb{P}}(0)-2\alpha_{\mathbb{P}}'(t)}. \quad (17)$$

It is worth to mention that the smallness of the triple-Pomeron coupling is related to the known shortness of gluon correlation length. The amplitude $q + g \rightarrow q + G$ is given by open circles as in Figure 3. So the 3-Pomeron term is interpreted as an excitation of the projectile proton due to the gluon radiation. The diffractive valence quark excitation is shown in Figure 5, graphs (bb) and (cb), and contributes to

$$\frac{d\sigma_{\text{diff}}^{\text{PPR}}}{d\xi dt} \propto \xi^{\alpha_{\mathbb{P}}(0)-\alpha_{\mathbb{P}}(0)-2\alpha_{\mathbb{P}}'(t)}. \quad (18)$$

3.2. Diffractive Factorization Breaking in Forward Diffraction. As an alternative to the diffractive factorization based approach, the dipole description of the QCD diffraction was presented in [11] (see also [40]). The color dipole description of inclusive Drell-Yan process was first introduced in [41] (see also [36, 42]) and treats the production of a heavy virtual photon via bremsstrahlung mechanism rather than $\bar{q}q$ annihilation. The dipole approach applied to diffractive DY reaction in [6, 7] and later in diffractive vector boson production [8] has explicitly demonstrated the diffractive factorization breaking in diffractive Abelian radiation reactions.

It is worth emphasizing that the quark radiating the gauge boson cannot be a spectator but must participate in the interaction. This is a straightforward consequence of the Good-Walker mechanism of diffraction [3]. According to this picture, diffraction vanishes if all Fock components of the hadron interact with the same elastic amplitudes. Then an unchanged Fock state composition emerges from the interaction; that is, the outgoing hadron is the same as the incoming one, so the interaction is elastic.

For illustration, consider diffractive photon radiation off a quark [23]. The relevant contributions and kinematics of the process are schematically presented in Figure 6 where the Pomeron exchange is depicted as an effective two-gluon (BFKL) ladder. The corresponding framework has previously been used for diffractive gluon radiation and diffractive DIS processes in [23, 43, 44] and we adopt similar notations in what follows. Applying the generalized optical theorem in the high energy limit with a cut between the ‘‘screening’’ and ‘‘active’’ gluon as shown by dashed line in Figure 6, we get

$$\begin{aligned} \widehat{A}_{\text{SD}} &= \frac{i}{2} \sum_{Y_8^*} \left[\widehat{A}^\dagger(q\gamma p \rightarrow q\{Y_8^*\}) \widehat{A}(qp \rightarrow q\{Y_8^*\}) \right. \\ &\quad \left. + \widehat{A}^\dagger(q\gamma p \rightarrow q\gamma\{Y_8^*\}) \widehat{A}(qp \rightarrow q\gamma\{Y_8^*\}) \right], \end{aligned} \quad (19)$$

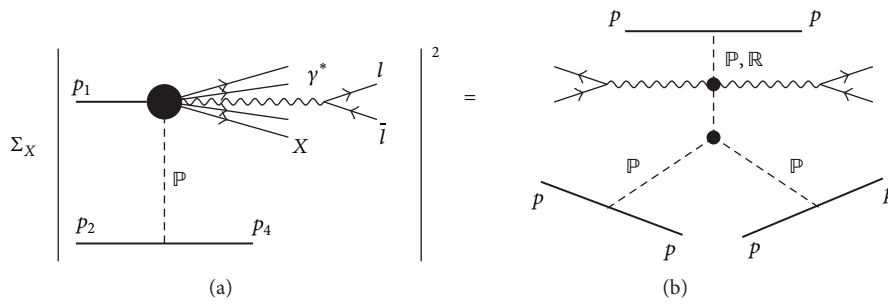


FIGURE 4: The diffractive DY cross section summed over excitation channels at fixed effective mass M_X (a). The latter corresponds to the Mueller graph in Regge picture (b).

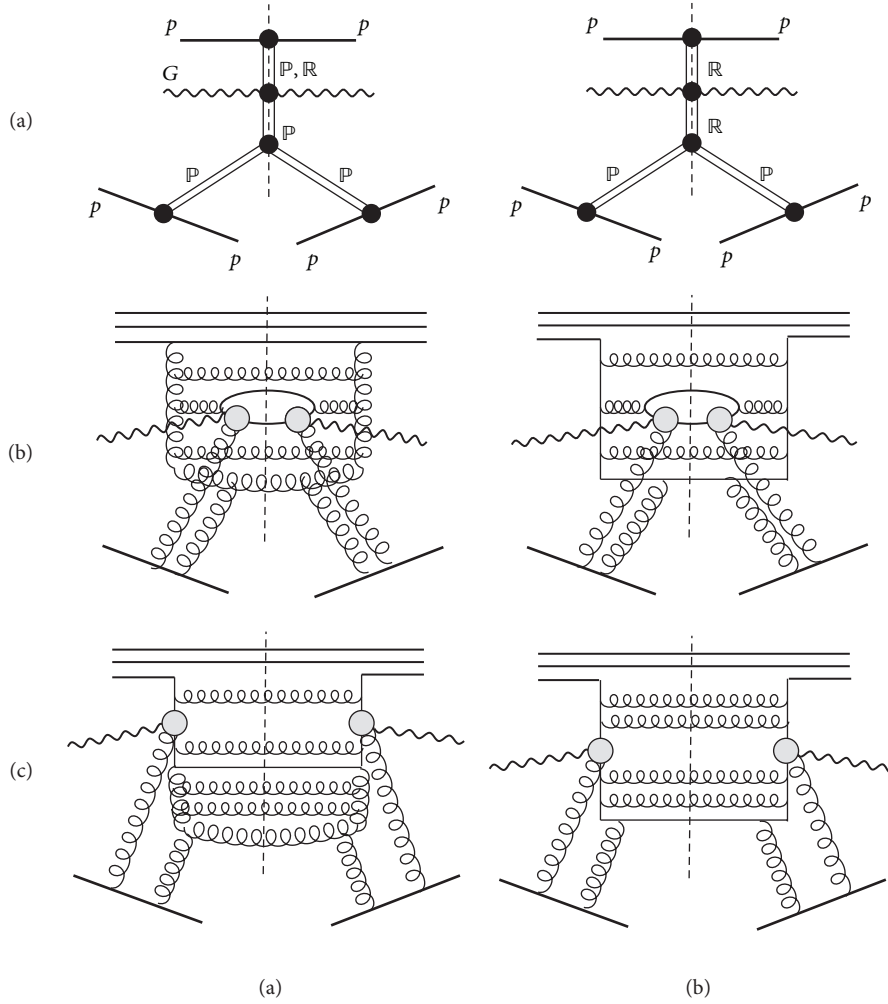


FIGURE 5: The upper row contains the triple-Regge graphs for $pp \rightarrow (XG^*) + p$. A few key examples of diagrams for diffractive excitation of a large invariant mass are given by 2nd and 3rd rows.

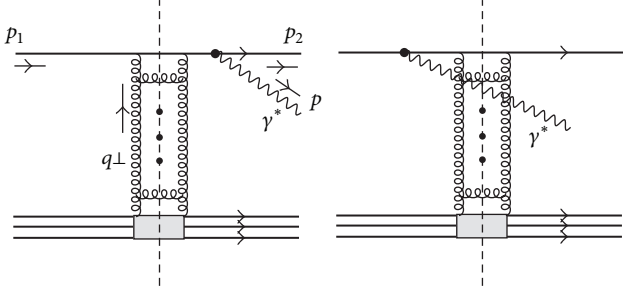


FIGURE 6: Schematic illustration of the typical contributions and kinematics of the diffractive Drell-Yan process in the quark-target collision.

with summation going through all octet-changed intermediate states $\{Y_8^*\}$. In (19), the first and second terms correspond to the first and second diagrams in Figure 6. Then we switch to impact parameter representation:

$$\widehat{A}(\vec{b}, \vec{r}) = \frac{1}{(2\pi)^4} \int d^2 \vec{q}_\perp d^2 \vec{\kappa} \widehat{A}(\vec{q}_\perp, \vec{\kappa}) e^{-i\vec{q}_\perp \cdot \vec{b} - i\vec{r} \cdot \vec{\kappa}}, \quad (20)$$

$$\vec{\kappa} = \alpha \vec{p}_2 - (1 - \alpha) \vec{p},$$

where \vec{q}_\perp , \vec{p}_2 , and \vec{p} are the transverse momenta of the Pomeron, final quark, and the radiated photon γ^* , α is the longitudinal momentum fraction of the photon taken off the parent quark p_1 , and κ is the relative transverse momentum between the final quark and γ^* . Thus, the amplitude of the “screening” gluon exchange summed over projectile valence quarks $j = 1, 2, 3$ reads as follows:

$$\begin{aligned} \widehat{A}(qp \rightarrow q\{Y_8^*\}) &= \sum_a \tau_a \langle f | \widehat{\gamma}_a(\vec{b}_1) | i \rangle, \\ \widehat{A}(q\gamma p \rightarrow q\gamma\{Y_8^*\}) &= \sum_a \tau_a \langle f | \widehat{\gamma}_a(\vec{b}_2) | i \rangle, \\ \widehat{A}(qp \rightarrow q\gamma\{Y_8^*\}) &= \widehat{A}(q\gamma p \rightarrow q\gamma\{Y_8^*\}) \\ &= \sum_a \tau_a [\langle f | \widehat{\gamma}_a(\vec{b}_1) | i \rangle - \langle f | \widehat{\gamma}_a(\vec{b}_2) | i \rangle] \\ &\cdot \Psi_{q \rightarrow q\gamma}(\vec{r}, \alpha), \end{aligned} \quad (21)$$

where $\vec{b}_1 \equiv \vec{b}$ and $\vec{b}_2 \equiv \vec{b} - \alpha \vec{r}$ are the impact parameter of the quark before and after photon radiation, \vec{r} is the transverse separation between the quark and the radiated photon, α is the momentum fraction taken by the photon, $\Psi_{q \rightarrow q\gamma}$ is the distribution function for the $q\gamma$ fluctuation of the quark, $\lambda_a = 2\tau_a$ are the Gell-Mann matrices from a gluon coupling to the quark, and matrices $\widehat{\gamma}_a$ are the operators in coordinate and color space for the target quarks:

$$\begin{aligned} \widehat{\gamma}_a(\vec{R}) &= \sum_i \tau_a^{(i)} \chi(\vec{R} - \vec{s}_i), \\ \chi(\vec{s}) &\equiv \frac{1}{\pi} \int d^2 q \frac{\alpha_s(q) e^{i\vec{q} \cdot \vec{s}}}{q^2 + \Lambda^2}, \end{aligned} \quad (22)$$

which depend on the effective gluon mass, $\Lambda \sim 100$ MeV, and on the transverse distance between i th valence quark in the target nucleon and its center of gravity, \vec{s}_i .

Combining these ingredients into the diffractive amplitude (19) one should average over color indices of the valence quarks and their relative coordinates in the target nucleon $|3q\rangle_1$. The color averaging results in

$$\langle \tau_a^{(j)} \cdot \tau_{a'}^{(j')} \rangle_{|3q\rangle_1} = \begin{cases} \frac{1}{6} \delta_{aa'} & : j = j' \\ -\frac{1}{12} \delta_{aa'} & : j \neq j'. \end{cases} \quad (23)$$

Finally, averaging over quark relative coordinates \vec{s}_i leads to

$$\langle i | \widehat{\gamma}_a(\vec{b}_k) \widehat{\gamma}_{a'}(\vec{b}_l) | i \rangle_{|3q\rangle_1} = \frac{3}{4} \delta_{aa'} S(\vec{b}_k, \vec{b}_l), \quad (24)$$

where $S(\vec{b}_k, \vec{b}_l)$ is a scalar function, which can be expressed in terms of the quark-target scattering amplitude $\chi(\vec{r})$ and the proton wave function [23]. Then, the total amplitude is

$$\widehat{A}(\vec{b}, \vec{r}) \propto S(\vec{b}, \vec{b}) - S(\vec{b} - \alpha \vec{r}, \vec{b} - \alpha \vec{r}). \quad (25)$$

After Fourier transform one notices that in the forward quark limit $q_\perp \rightarrow 0$ the amplitude for single diffractive photon or any Abelian radiation vanishes, $A(\vec{q}_\perp, \kappa)|_{q_\perp \rightarrow 0} = 0$, and

$$\left. \frac{d\sigma_{sd}^{DY}}{d\alpha d^2 q_T^2} \right|_{q_T=0} = 0, \quad (26)$$

in accordance with the Landau-Pomeranchuk principle. Indeed, in both Fock components of the quark, $|q\rangle$ and $|q\gamma^*\rangle$, only the quark interacts, so these components interact equally and thus no diffraction is possible. One immediately concludes that the diffractive factorization must be strongly broken.

The function $S(\vec{b}_k, \vec{b}_l)$ above is directly related to $q\bar{q}$ dipole cross section as

$$\begin{aligned} \sigma_{q\bar{q}}(\vec{r}_1 - \vec{r}_2) &\equiv \int d^2 b [S(\vec{b} + \vec{r}_1, \vec{b} + \vec{r}_1) \\ &+ S(\vec{b} + \vec{r}_2, \vec{b} + \vec{r}_2) - 2S(\vec{b} + \vec{r}_1, \vec{b} + \vec{r}_2)]. \end{aligned} \quad (27)$$

Thus, following analogical scheme one can obtain the diffractive amplitude of any diffractive process as a linear combination of the dipole cross sections for different dipole separations. As was anticipated, the diffractive amplitude represents the destructive interference effect from scattering of dipoles of slightly different sizes. Such an interference results in an interplay between hard and soft fluctuations in the diffractive pp amplitude, contributing to breakdown of diffractive factorization.

When one considers diffractive DY off a finite-size object like a proton, in both Fock components, $|3q\rangle$ and $|3q\gamma^*\rangle$, only the quark hadron-scale dipoles interact. These dipoles are large due to soft intrinsic motion of quarks in the projectile proton wave function. The dipoles, however, have different sizes, since the recoil quark gets a shift in impact parameters.

So the dipoles interact differently giving rise to forward diffraction. The contribution of a given projectile Fock state to the diffraction amplitude is given by the difference of elastic amplitudes for the Fock states including and excluding the gauge boson:

$$\text{Im } f_{\text{diff}}^{(n)} = \text{Im } f_{\text{el}}^{(n+G)} - \text{Im } f_{\text{el}}^{(n)}, \quad (28)$$

where n is the total number of partons in the Fock state and $f_{\text{el}}^{(n+G)}$ and $f_{\text{el}}^{(n)}$ are the elastic scattering amplitudes for the whole n -parton ensemble, which either contains the gauge boson or does not, respectively. Although the gauge boson does not participate in the interaction, the impact parameter of the quark radiating the boson gets shifted, and this is the only reason why the difference (28) is not zero (see the next section). This also conveys that this quark must interact in order to retain the diffractive amplitude nonzero [6, 7]. For this reason in the graphs depicted in Figure 5 the quark radiating G always takes part in the interaction with the target.

Notice that there is no one-to-one correspondence between diffraction in QCD and the triple-Regge phenomenology. In particular, there is no triple-Pomeron vertex localized in rapidity. The colorless ‘‘Pomeron’’ contains at least two t -channel gluons, which can couple to any pair of projectile partons. For instance, in diffractive gluon radiation, which is the lowest order term in the triple-Pomeron graph, one of the t -channel gluons can couple to the radiated gluon, while another one couples to another parton at any rapidity, for example, to a valence quark (see Figure 3 in [23]). Apparently, such a contribution cannot be associated literally with either of the Regge graphs in Figure 5. Nevertheless, this does not affect much x_F and energy dependencies provided by the triple-Regge graphs, because the gluon has spin one.

It is also worth mentioning that in Figure 5 we presented only the lowest order graphs with two-gluon exchange. The spectator partons in a multiparton Fock component also can interact and contribute to the elastic amplitude of the whole parton ensemble. This gives rise to higher order terms, not shown explicitly in Figure 5. They contribute to the diffractive amplitude (28) as a factor, which we define as the gap survival amplitude [8].

As was mentioned above the amplitude of diffractive gauge boson radiation by a quark-antiquark dipole does not vanish in forward direction, unlike the radiation by a single quark [6, 23]. This can be understood as follows. According to the general theory of diffraction [1–3, 5], the off-diagonal diffractive channels are possible only if different Fock components of the projectile (eigenstates of interaction) interact with different elastic amplitudes. Clearly, the two Fock states consisting of just a quark and of a quark plus a gauge boson interact equally, if their elastic amplitudes are integrated over impact parameter. Indeed, when a quark fluctuates into a state $|qG\rangle$ containing the gauge boson G , with the transverse quark-boson separation \vec{r} , the quark gets a transverse shift $\Delta\vec{r} = \alpha\vec{r}$. The impact parameter integration gives the forward amplitude. Both Fock states $|q\rangle$ and $|qG\rangle$ interact with the target with the same total cross section; this is why a quark cannot radiate at zero-momentum transfer and

hence G is not produced diffractively in the forward direction. This is the general and model independent statement. The details of this general consideration can be found in [23] (Appendices A 1 and A 4). The same result is obtained calculating Feynman graphs in Appendix B 4 of the same paper. Unimportance of radiation between two interactions was also demonstrated by Brodsky and Hoyer in [45].

Note that in all these calculations one assumes that the coherence time of radiation considerably exceeds the time interval between the two interactions, which is fulfilled in our case, since we consider radiation at forward rapidities. The disappearance of both inelastic and diffractive forward Abelian radiation has a direct analogy in QED: if the electric charge gets no ‘‘kick,’’ that is, not accelerated, no photon is radiated, provided that the radiation time considerably exceeds the duration time of interaction. This is dictated by the renowned Landau-Pomeranchuk principle [46]: radiation depends on the strength of the accumulated kick, rather than on its structure, if the time scale of the kick is shorter than the radiation time. It is worthy to notice that the non-Abelian QCD case is different: a quark can radiate gluons diffractively in the forward direction. This happens due to a possibility of interaction between the radiated gluon and the target. Such a process, in particular, becomes important in diffractive heavy flavor production [9].

The situation changes if the gauge boson is radiated diffractively by a dipole as shown in Figure 7. Then the quark dipoles with or without a gauge boson have different sizes and interact with the target differently. So the amplitude of the diffractive gauge boson radiation from $q\bar{q}$ dipole is proportional to the difference between elastic amplitudes of the two Fock components, $|q\bar{q}\rangle$ and $|q\bar{q}G\rangle$ [6]; that is,

$$M_{q\bar{q}}^{\text{diff}}(\vec{b}, \vec{R}, \vec{r}, \alpha) \propto \Psi_{q \rightarrow G^*q}(\alpha, \vec{r}) \cdot [2 \text{Im } f_{\text{el}}(\vec{b}, \vec{R}) - 2 \text{Im } f_{\text{el}}(\vec{b}, \vec{R} + \alpha\vec{r})], \quad (29)$$

where $\Psi_{q \rightarrow G^*q}$ is the light-cone (nonnormalised) wave function of $q \rightarrow G^*q$ fluctuation corresponding to bremsstrahlung of virtual gauge bosons $G = \gamma, Z, W^\pm$ of mass M [8], $\vec{R} = \vec{r}_1 - \vec{r}_2$ is the transverse size of the $q\bar{q}$ dipole, α is the momentum fraction of the gauge boson G taken off the parent quark q , and $r \sim 1/M$ is the hard scale.

When applied to diffractive pp scattering the diffractive amplitude (29), thus, occurs to be sensitive to the large transverse separations between the projectile quarks in the incoming proton. Normally, transition to the hadron level is achieved by using the initial proton Ψ_i and remnant Ψ_f wave functions which encode information about distributions of constituents. The completeness relation to the wave function of the unobservable proton remnant is

$$\sum_{\text{fin}} \Psi_{\text{fin}}(\vec{r}_1, \vec{r}_2, \vec{r}_3; \{x_q^{1,2,\dots}\}, \{x_g^{1,2,\dots}\}) \cdot \Psi_{\text{fin}}^*(\vec{r}'_1, \vec{r}'_2, \vec{r}'_3; \{x_q'^{1,2,\dots}\}, \{x_g'^{1,2,\dots}\}) = \delta(\vec{r}_1 - \vec{r}'_1) \cdot \delta(\vec{r}_2 - \vec{r}'_2) \delta(\vec{r}_3 - \vec{r}'_3) \prod_j \delta(x_{q/g}^j - x_{q/g}'^j). \quad (30)$$

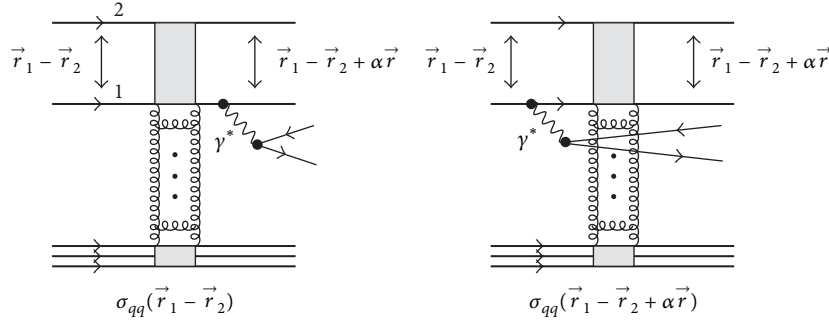


FIGURE 7: Leading order contribution to the diffractive Drell-Yan in the dipole-target collision.

Here, $\vec{r}_{q/g}^i$ and $x_{q/g}^i$ are the coordinates and fractional momenta of the valence/sea partons.

Since gluons and sea quarks are mostly accumulated in a close vicinity of valence quarks (inside gluonic “spots”), to a reasonable accuracy the transverse positions of sea quarks and gluons can be identified with the coordinates of valence quarks. The valence part of the wave function is often taken to be a Gaussian distribution such that

$$|\Psi_{\text{in}}|^2 = \frac{3a^2}{\pi^2} e^{-a(r_1^2+r_2^2+r_3^2)} \mathcal{R}(x_1, \{x_q^{1,2,\dots}\}, \{x_g^{2,3,\dots}\}) \cdot \delta(\vec{r}_1 + \vec{r}_2 + \vec{r}_3) \delta\left(1 - x_1 - \sum_j x_{q/g}^j\right), \quad (31)$$

where all the partons not participating in the hard interaction are summed up, x_1 is the photon fraction taken from the initial proton, $a = \langle r_{\text{ch}}^2 \rangle^{-1}$ is the inverse proton mean charge radius squared, and \mathcal{R} is a collinear multiparton distribution in the proton. Once the latter is integrated over all the partons not participating in the hard interaction, one gets a conventional collinear PDF $g(x_1, \mu^2)$ for gluons and $q(x_1, \mu^2)$ for a given quark flavor q . Since the diffractive pp cross section appears as a sum of diffractive excitations of the proton constituents, valence/sea quarks and gluons are incorporated as

$$|\Psi_{\text{in}}(\vec{r}_i, x_i)|^2 \propto \frac{1}{3} \left[\sum_q q(x) + \bar{q}(x) + \frac{81}{16} g(x) \right], \quad (32)$$

after integration over spectator impact parameters and momentum fractions with a proper color factor between quark and gluon PDFs. Note that only sea and valence quarks are excited by the photon radiation in the diffractive DY process which provide a direct access to the proton structure function in the soft limit of large x [36]:

$$\sum_q Z_q^2 [q(x) + \bar{q}(x)] = \frac{1}{x} F_2(x). \quad (33)$$

For diffractive gluon radiation one should account for both quark and gluon excitations whose amplitudes, however, are calculated in different ways [23].

Due to the internal transverse motion of the projectile valence quarks inside the incoming proton, which corresponds to finite large transverse separations between them,

the forward photon radiation does not vanish [6, 8]. These large distances are controlled by a nonperturbative (hadron) scale \vec{R} , such that the diffractive amplitude has the Good-Walker structure:

$$M_{\bar{q}q}^{\text{diff}} \propto \sigma(\vec{R}) - \sigma(\vec{R} - \alpha\vec{r}) \propto \vec{r} \cdot \vec{R}, \quad (34)$$

while the single diffractive-to-inclusive cross sections ratio behaves as

$$\frac{\sigma_{\text{sd}}^{\text{DY}}}{\sigma_{\text{incl}}^{\text{DY}}} \propto \frac{\exp(-2R^2/R_0^2(x_2))}{R_0^2(x_2)} \quad (35)$$

assuming the saturated GBW shape of the dipole cross section (9), where x_2 is defined in (14). Thus, the soft part of the interaction is not enhanced in Drell-Yan diffraction which is semihard/semisoft like inclusive DIS. Linear dependence on the hard scale $r \sim 1/M \ll R_0(x_2)$ means that even at a hard scale the Abelian radiation is sensitive to the hadron size due to a dramatic breakdown of diffractive factorization [37]. It was firstly found in [47, 48] that factorization for diffractive Drell-Yan reaction fails due to the presence of spectator partons in the Pomeron. In [6–8] it was demonstrated that factorization in diffractive Abelian radiation is thus even more broken due to presence of spectator partons in the colliding hadrons as reflected in (34).

The effect of diffractive factorization breaking manifests itself in specific features of observables like a significant damping of the cross section at high \sqrt{s} compared to the inclusive production case as illustrated in Figure 8. This is rather unusual, since a diffractive cross section, which is proportional to the dipole cross section squared, could be expected to rise with energy steeper than the total inclusive cross section, like it occurs in the diffractive DIS process. At the same time, the ratio of DDY to DY cross sections was found in [6, 7] to rise with the hard scale, and the photon virtuality M^2 was also shown in Figure 8. This is also in variance with diffraction in DIS, which is associated with the soft interactions and where the diffractive factorization holds true [10].

Such striking signatures of the diffractive factorization breaking are due to an interplay of soft and hard interactions in the corresponding diffractive amplitude. Namely, large and small size projectile fluctuations contribute to the diffractive Abelian radiation process on the same footing providing the

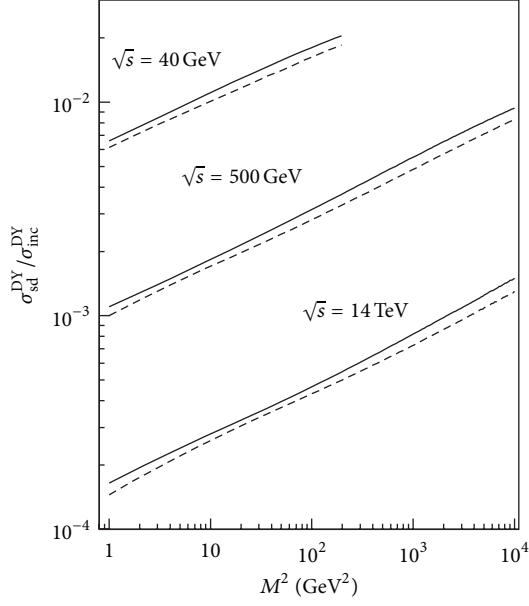


FIGURE 8: The single diffractive-to-inclusive DY cross sections ratio as a function of the photon virtuality M^2 for $x_1 = 0.5$ (solid lines) and $x_1 = 0.9$ (dashed lines) and c.m.s. energies $\sqrt{s} = 40$ GeV, 500 GeV, and 14 TeV (from top to bottom) [6].

leading twist nature of the process, whereas diffractive DIS dominated by soft fluctuations only is of higher twist [6, 7]. But this is not the only source of the factorization breaking; another important source is the absorptive (or unitarity) corrections.

3.3. Gap Survival Amplitude. In the limit of unitarity saturation (the so-called black-disk limit) the absorptive corrections can entirely terminate the large rapidity gap process. The situation close to this limit, in fact, happens in high energy (anti)proton-proton collisions such that unitarity is nearly saturated at small impact parameters [49, 50]. The unitarity corrections are typically parameterized by a suppression factor also known as the soft survival probability which significantly reduce the diffractive cross section. In hadronic collisions this probability is controlled by the soft spectator partons which are absent in the case of diffractive DIS causing the breakdown of diffractive factorization.

It is well known that the absorptive corrections affect differently the diagonal and off-diagonal terms in the hadronic current [5, 51], in opposite directions, leading to an additional source of the QCD factorization breaking in processes with off-diagonal contributions only. Namely, the absorptive corrections enhance the diagonal terms at larger \sqrt{s} , whereas they strongly suppress the off-diagonal ones. In the diffractive DY process a new state, the heavy lepton pair, is produced; hence, the whole process is of entirely off-diagonal nature, whereas the diffractive DIS process contains both diagonal and off-diagonal contributions [5].

Amplitude (29) is the full expression, which includes by default the effect of absorption and does not need any extra survival probability factor [8]. This can be illustrated in a

simple example of elastic dipole scattering off a potential. In this case, the dipole elastic amplitude has the eikonal form:

$$\text{Im } f_{\text{el}}(\vec{b}, \vec{r}_1 - \vec{r}_2) = 1 - \exp [i\chi(\vec{r}_1) - i\chi(\vec{r}_2)], \quad (36)$$

where

$$\chi(b) = - \int_{-\infty}^{\infty} dz V(\vec{b}, z) \quad (37)$$

and $V(\vec{b}, z)$ is the potential, which depends on the impact parameter and longitudinal coordinate, and is nearly imaginary at high energies. The difference between elastic amplitudes with a shifted quark position, which enters the diffractive amplitude, reads as follows:

$$\begin{aligned} & \text{Im } f_{\text{el}}(\vec{b}, \vec{r}_1 - \vec{r}_2 + \alpha\vec{r}) - \text{Im } f_{\text{el}}(\vec{b}, \vec{r}_1 - \vec{r}_2) \\ & \simeq \exp [i\chi(\vec{r}_1) - i\chi(\vec{r}_2)] \exp [i\alpha\vec{r} \cdot \vec{\nabla}\chi(\vec{r}_1)]. \end{aligned} \quad (38)$$

Here, the first factor $\exp[i\chi(\vec{r}_1) - i\chi(\vec{r}_2)]$ is exactly the survival probability amplitude, which vanishes in the black disc limit, as it should do. This proves that the diffractive amplitude (29) includes the effect of all absorptive corrections (gap survival amplitude), provided that the dipole cross section is adjusted to the data. Note that usually the survival probability factor is introduced into the diffractive cross section probabilistically, while in (29) it is treated quantum-mechanically, at the amplitude level.

The diffractive gluon radiation is known to be rather weak (the 3-Pomeron coupling is small). This phenomenological observation can be explained assuming that gluons in the proton are predominantly located inside small ‘‘gluonic spots’’ of size $r_0 \sim 0.3$ fm around the valence quarks (see, e.g., [23, 52–54]). The smallness of gluonic dipole is an important nonperturbative phenomenon which may be connected, for example, to the small size of gluonic fluctuations in the instanton liquid model [53]. Therefore, a distance between a valence quark and a gluon in a vicinity of another quark can be safely approximated by the quark-quark separation.

Besides the soft gluons in the proton light-cone wave function, virtual gauge boson production triggers intensive gluon radiation such that there are many more spectator gluons in a vicinity of the quark which radiates the gauge boson. The separations of such gluons from the parent quark are controlled by the QCD DGLAP dynamics. In practice, one may replace such a set of gluons by dipoles [55] whose transverse sizes r_d vary between $1/M_G$ and r_0 scales [56]. Then the mean dipole size is regulated by a relation:

$$\langle r_d^2 \rangle = \frac{r_0^2}{\ln(r_0^2 M_G^2)}, \quad (39)$$

leading to $\langle r_d^2 \rangle \approx 0.01$ fm², which means that it is rather small and the corresponding dipole cross section $\sigma \approx C(x)\langle r_d \rangle^2$, where $C(x) = \sigma_0/R_0^2(x)$ rises with energy, is suppressed. For $x = M_G^2/s$ and naive GBW parameterization [26] we get $\sigma \approx 0.9$ mb at the Tevatron energy. Each such small dipole

brings up an extra suppression factor to the large rapidity gap survival amplitude given by

$$S_d(s) = 1 - \text{Im } f_d(b, r_d). \quad (40)$$

Here, the second term is small and thus is simplified to (for more details, see [57])

$$\text{Im } f_d(b, r_d) \approx \frac{\sigma_d}{4\pi B_d} e^{-b^2/2B_d}, \quad (41)$$

where B_d is the standard dipole-nucleon elastic slope $B_d \approx 6 \text{ GeV}^{-2}$ measured earlier in diffractive ρ electroproduction at HERA [58]. At the mean impact parameter given by $\langle b^2 \rangle = 2B_d$ and for the Tevatron energy $\sqrt{s} = 2 \text{ TeV}$ we arrive at negligibly small value for the absorptive correction (41): $\text{Im } f_d(0, r_d) \approx 0.01$.

On the other hand, the overall number of such dipoles increases with hardness of the process, which can amplify the magnitude of the absorptive effect. Generalizing the gap survival amplitude to n_d projectile dipoles, we obtain

$$S_d^{(n_d)} = [1 - \text{Im } f_d(b, r_d)]^{n_d}. \quad (42)$$

The DGLAP evolution formulated in impact parameter representation [56] enables estimating that the mean number of such dipoles can be estimated in the double-leading-log approximation:

$$\langle n_d \rangle = \sqrt{\frac{12}{\beta_0} \ln\left(\frac{1}{\alpha_s(M_G^2)}\right) \ln\left((1-x_F)\frac{s}{s_0}\right)}. \quad (43)$$

Here, the typical Bjorken x values of the radiated gluons are restricted by the diffractive mass as $x > s_0/M_X^2 = s_0/(1-x_F)s$. In typical kinematics at the Tevatron collider, the mean number of such dipoles is roughly $\langle n_d \rangle \lesssim 6$. The amplitude of survival of a large rapidity gap is controlled by the largest dipoles in the projectile hadron only, such that the first exponential factor in (38) provides a sufficiently good approximation to the gap survival amplitude. The absorptive corrections (42) to the gap survival amplitude are proven to be rather weak and do not exceed 5% (or 10% in the survival probability factor) which is small compared to an overall theoretical uncertainty. For the pioneering work on hard rescattering corrections to the gap survival factor see [59].

The popular quasi-eikonal model for the so-called ‘‘enhanced’’ probability \widehat{S}_{enh} (see, e.g., [21, 59]), frequently used to describe the factorization breaking in diffractive processes, is not well justified in higher orders, whereas the color dipole approach, considered here, correctly includes all diffraction excitations to all orders [5]. Such effects are included into the phenomenological parameterizations for the partial elastic dipole amplitude fitted to data. This allows predicting the diffractive gauge bosons production cross sections in terms of a single parameterization for the universal dipole cross section (or, equivalently, the elastic dipole amplitude) known independently from the soft hadron scattering data.

For more details on derivations of diffractive gauge boson production amplitudes and cross sections see [7, 8]. Now we turn to a discussion of numerical results for the most important observables.

4. Single Diffractive Gauge Bosons Production

In [8] the dipole framework has been used in analysis of single diffractive gauge bosons production, and here we briefly overview these results. The corresponding cross sections for Z^0, γ^* , and W^\pm bosons production ($\sqrt{s} = 14 \text{ TeV}$), differential in the lepton pair mass squared $d\sigma_{\text{sd}}/dM^2$, and its longitudinal momentum fraction, $d\sigma_{\text{sd}}/dx_1$, are shown in Figures 9(a) and 9(b), respectively. M^2 distributions here are integrated over the forward rapidities (i.e., $0.3 < x_1 < 1$) while the invariant mass distribution is integrated over $5 < M^2 < 10^5 \text{ GeV}^2$.

In the resonants Z^0 and W^\pm region the M^2 distributions exceed the corresponding DDY component; only for low masses γ^* contribution becomes important. As for x_1 distribution, the diffractive W^+ and γ^* components are comparable to each other, whereas W^- and Z -boson production cross section are much lower. A precision measurement of differences in forward diffractive W^+ and W^- rates may enable further constraining of the quark content of the proton at large fractions $x_q \equiv x_1/\alpha$.

Another phenomenologically interesting observable is the lepton pair transverse momentum q_\perp distribution at the LHC shown in Figure 10(a) at the corresponding Z or W resonance. One of the important observables, sensitive to the difference between u - and d -quark PDFs at large x , W^\pm charge asymmetry is defined as

$$A_W(x_1) = \frac{d\sigma_{\text{sd}}^{W^+}/dx_1 - d\sigma_{\text{sd}}^{W^-}/dx_1}{d\sigma_{\text{sd}}^{W^+}/dx_1 + d\sigma_{\text{sd}}^{W^-}/dx_1}. \quad (44)$$

And it is shown in Figure 10(b). The quantity is independent of both M^2 and \sqrt{s} .

Similarly to diffractive DY discussed above, an important feature of the SD-to-inclusive gauge boson radiation cross sections ratio is

$$R(M^2, x_1) = \frac{d\sigma_{\text{sd}}/dx_1 dM^2}{d\sigma_{\text{incl}}/dx_1 dM^2}, \quad (45)$$

which is different from the one obtained in conventional diffractive QCD factorization-based approaches [18, 19] due to its unusual energy and scale dependence shown in Figure 11. In analogy to DDY case, this ratio behaves with respect to the energy and the hard scale in opposite way to what is expected from diffractive factorization. The ratio appears to be independent of the gauge boson properties and quark PDFs and is sensitive only to the structure of the universal elastic dipole amplitude. This means it can be efficiently used as a probe for the QCD diffractive mechanism. Therefore, measurements of the single diffractive gauge boson production cross section in the dilepton channel which enhanced compared to DDY around the Z^0 and W^\pm resonances would provide important information about the interplay between soft and hard interactions in QCD.

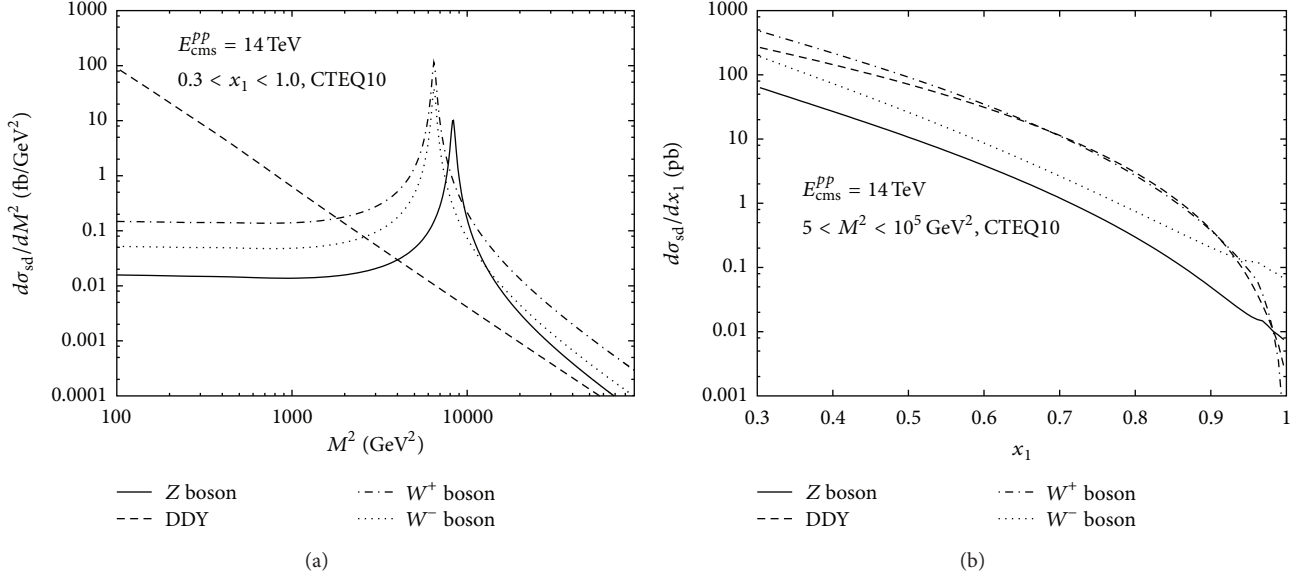


FIGURE 9: Diffractive gauge boson production cross section as function of invariant mass squared M^2 (a) and momentum fraction x_1 (b) at the LHC.

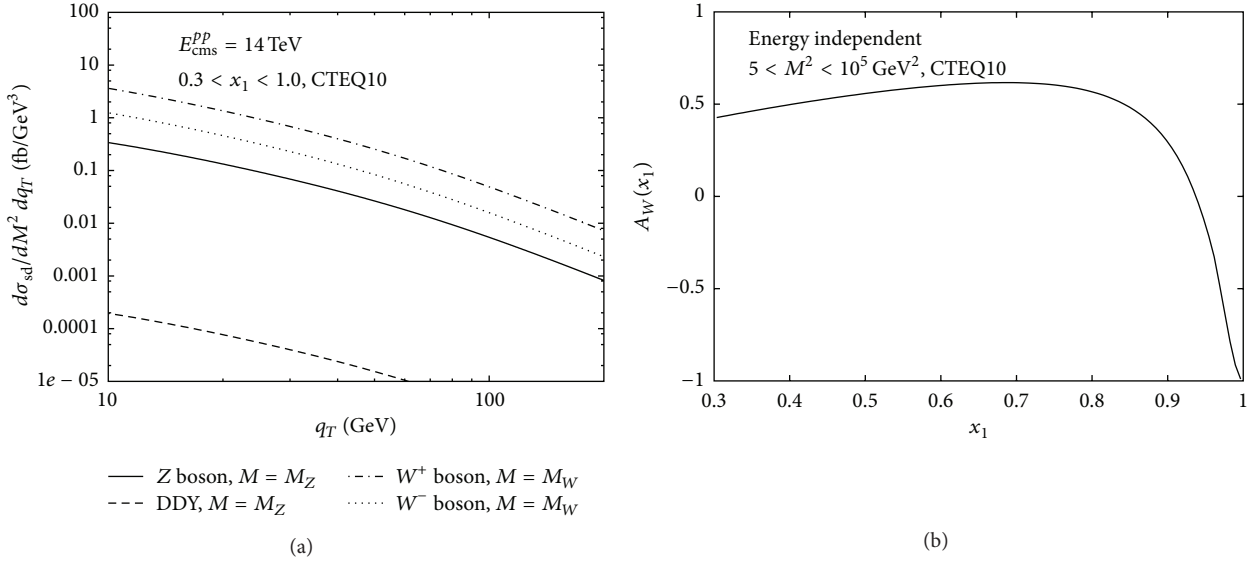


FIGURE 10: The lepton pair transverse momentum q_T distribution of the diffractive cross section at LHC $\sqrt{s} = 14$ TeV (a) and the charge asymmetry in SD W^\pm cross sections at fixed $M^2 = M_W^2$ (b).

5. Diffractive Non-Abelian Radiation

As we have seen in the discussion above, diffractive DY is one of the most important examples of leading twist processes, where simultaneously large and small size projectile fluctuations are at work. It turns out that the participation of soft spectator partons in the interaction with the gluonic ladder is crucial and results in a leading twist effect. What are other examples of the leading twist behavior in diffraction?

5.1. Leading Twist Diffractive Heavy Flavor Production. One might naively think that the Abelian (or DIS) mechanism of

heavy flavor production $\gamma^* \rightarrow Q\bar{Q}$ is of the leading twist as well since it behaves as $\sim 1/Q^2$. However, in the limit $m_Q^2 \gg Q^2$ the corresponding cross section $\sigma_{sd} \propto 1/m_Q^4$, that is, behaving as a higher twist process. One has to radiate at least one gluon off $Q\bar{Q}$ pair for this process to become the leading twist one, for example, $\sigma_{sd}(\gamma^* \rightarrow Q\bar{Q}g) \propto 1/m_Q^2$, since the mean transverse separation between G and small $Q\bar{Q}$ dipole is typically large although formally such a process is of the higher perturbative QCD order in α_s .

Consider now the non-Abelian mechanism for diffractive hadroproduction of heavy quarks via $g^* \rightarrow Q\bar{Q}$ hard

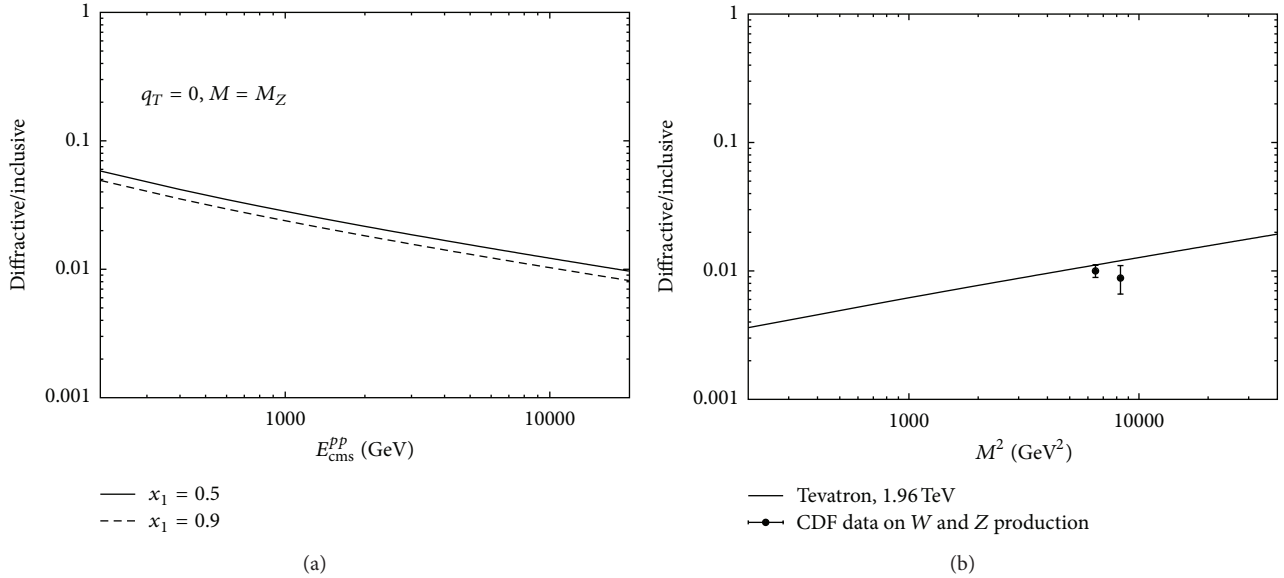


FIGURE 11: The SD-to-inclusive ratio of the gauge bosons production cross sections as a function of the c.m. energy \sqrt{s} (a) and the lepton pair invariant mass M^2 at the Tevatron (b).

subprocess. Production of heavy quarks at large $x_F \rightarrow 1$ is a longstanding controversial issue even in inclusive processes. On one hand, QCD factorization approach predicts vanishingly small yields of heavy flavor due to steeply falling gluon density as $\sim (1 - x_F)^5$ at large x_F . On the other hand, the endpoint behavior is controlled by the universal Regge asymptotics $d\sigma/dx_F(x_F \rightarrow 1) \propto (1 - x_F)^{1-2\alpha_R(t)}$ in terms of the Regge trajectory of the t -channel exchange $\alpha_R(t)$. Apparently, the Regge and QCD factorization approaches contradict each other. The same problem emerges in the DY process at large x_F as is seen in data [60] which means that in the considered kinematics the conventional QCD factorization does not apply [61]. At the same time, the observation of an excess of diffractive production of heavy quarks at large $x_F \rightarrow 1$ compared to conventional expectation may provide a good evidence for intrinsic heavy flavors if the latter is reliably known. Calculations assuming that diffractive factorization holds for hard diffraction [12, 39] may not be used for quantifying the effect from intrinsic heavy flavor. Instead, the dipole framework has been employed to this process for the first time in [9]. Here we briefly overview the basic theory aspects concerning primarily heavy quarks produced in the projectile fragmentation region (for inclusive $Q\bar{Q}$ production at mid rapidities in the dipole framework, see [62]).

Typical contributions to the single diffractive $Q\bar{Q}$ production rate are summarized in Figure 12. Figures 12(a) and 12(b) correspond to the leading order gluon splitting into $Q\bar{Q}$ contributions in the color field of the target proton (diffractive gluon excitation). The latter gluon as a component of the projectile proton wave function can be treated as real (via collinear gluon PDF) or virtual (via unintegrated gluon PDF). Due to hard scale m_Q Figure 12(a) with Pomeron coupling to a small-size $gQ\bar{Q}$ system is of the higher twist due to

color transparency and is therefore suppressed. Figure 12(b) involves two scales: the soft hadronic one $\sim \Lambda_{\text{QCD}}$ associated with large transverse separations between a gluon and constituent valence quarks and the hard one $\sim m_Q$ associated with small $Q\bar{Q}$ dipole. An interplay between these two scales similar to that in DDY emerges as the leading twist effect; thus, Figure 12(b) is important. Possible higher order terms with an extra gluon radiation contributing to the leading twist diffractive heavy flavor production were discussed in detail in [9].

Figures 12(c) and 12(d) account for $Q\bar{Q}$ production via diffractive quark excitation. Just as in leading twist diffraction in DIS $\gamma^* \rightarrow Q\bar{Q}g$, these processes are associated with two characteristic transverse separations, a small one, $\sim 1/m_Q$, between the \bar{Q} and Q , and a large one, either $\sim 1/m_q$ between q and $Q\bar{Q}$ (Figure 12(c)) or $1/\Lambda_{\text{QCD}}$ between another constituent valence quark and $Q\bar{Q}$ (Figure 12(d)). While all the terms contributing to Figure 12(d) are of the leading twist (see [9]), only a special subset of Figure 12(c) are of the leading twist. Indeed, the hard subprocess $q + g \rightarrow (Q\bar{Q}) + q$ is characterized by five distinct topologies illustrated in Figure 13, and similar graphs are for gluon-proton scattering with subprocess $g + g \rightarrow (Q\bar{Q}) + g$.

These graphs can be grouped into two amplitudes attributed to bremsstrahlung (BR) and production (PR) mechanisms, which do or do not involve the projectile light quarks or gluons, respectively (for more details, see Figure 2 and Appendix A in [9]). The BR mechanism includes the same graphs as radiation of a gluon (see [43, 63]), that is, interaction with the source parton before and after radiation and interaction with the radiated gluon. The PR mechanism, responsible for the transition $g \rightarrow Q\bar{Q}$, includes

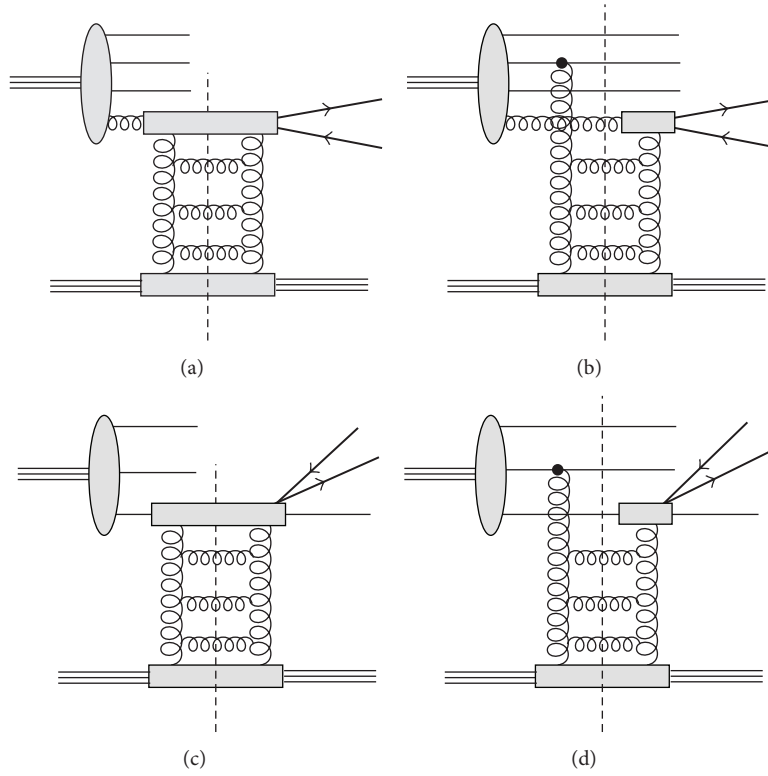


FIGURE 12: Leading order contributions to single diffractive heavy flavor production in gluon-proton (a, b) and quark-proton (c, d) scattering subprocesses in pp collisions. Diagrams (b, d) emerge due to the presence of soft spectator partons in the proton wave function (the screening gluon couples to every spectator parton besides the active one). Grey effective vertices account for all possible couplings of the incident partons.

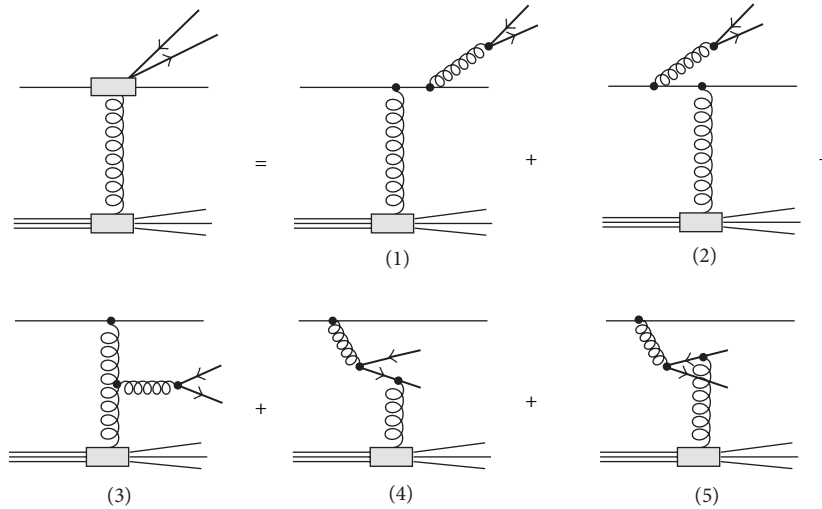


FIGURE 13: Five different topologies contributing to inclusive $Q\bar{Q}$ production in quark-proton scattering. These can be split into two gauge-invariant subsets of amplitudes as described in the text.

the interactions with the gluon and the produced $Q\bar{Q}$ (also known as gluon-gluon fusion $gg \rightarrow Q\bar{Q}$ mechanism). The total amplitude is

$$M_{q,g} = M_{q,g}^{\text{BR}} + M_{q,g}^{\text{PR}}, \quad (46)$$

where subscripts q, g denote contributions with hard gluon radiation by the projectile valence or sea quarks and gluons, respectively. Such grouping is performed separately for transversely and longitudinally polarised gluons as described in [9]. One of the reasons for this grouping is that each of these two combinations is gauge invariant and can be expressed

in terms of three-body dipole cross sections, $\sigma_{g\bar{q}q}$ and $\sigma_{g\bar{Q}Q}$, respectively.

Another physical reason for such a separation is different scale dependence of the BR and PR components. Introducing the transverse separations \vec{r} , \vec{r}_1 , and \vec{r}_2 within the $\bar{Q}Q$, $q\bar{Q}$, and qQ pairs, respectively, the three-body dipole cross sections can be expressed via two scales: the distance between the final light quark (or gluon) and the center of gravity of the $\bar{Q}Q$ pair, $\vec{\rho} = \vec{r} - \beta\vec{r}_1 - (1 - \beta)\vec{r}_2$ (β is the heavy quark momentum fraction taken from the parent gluon which takes fraction α of the parent parton) and the $\bar{Q}Q$ transverse separation, $\vec{s} = \vec{r}_1 - \vec{r}_2$. The corresponding distribution amplitudes of $\bar{Q}Q$ production in diffractive quark/gluon scattering off proton

$$\begin{aligned} A_{\text{BR}} &\propto \Phi_{\text{BR}}(\vec{\rho}, \vec{s}) \Sigma_1(\vec{\rho}, \vec{s}), \\ A_{\text{PR}} &\propto \Phi_{\text{PR}}(\vec{\rho}, \vec{s}) \Sigma_2(\vec{\rho}, \vec{s}) \end{aligned} \quad (47)$$

are given in terms of the effective dipole cross sections for colorless $g\bar{q}q$ and $g\bar{Q}Q$ systems and rather complicated wave functions Φ of subsequent gluon radiation and then its splitting into $\bar{Q}Q$ pair in both cases. In the case of bremsstrahlung, both mean separations are controlled by the hard scale such that

$$A_{\text{BR}} \sim \langle \rho^2 \rangle \sim \langle s^2 \rangle \sim \frac{1}{m_Q^2}, \quad (48)$$

and, thus, the corresponding contribution is a higher twist effect and thus suppressed (note that in the case of forward Abelian radiation this contribution is equal to zero). On the contrary, in the production mechanism only the $\bar{Q}Q$ separation is small, $\langle s^2 \rangle \sim 1/m_Q^2$; the second scale appears to be soft, $\langle \rho^2 \rangle \sim 1/m_q^2$, leading to the leading twist behavior

$$A_{\text{PR}} \sim \vec{s} \cdot \vec{\rho} \quad (49)$$

in analogy to diffractive DY process. This is a rather nontrivial fact, since in the case of the DY reaction such a property is due to the Abelian nature of the radiated particle while here we consider a non-Abelian radiation. The bremsstrahlung-production interference terms are of the higher twist and thus are safely omitted.

The situation with scale dependence in the case of $\bar{Q}Q$ production in diffractive pp scattering is somewhat similar to diffractive quark-proton scattering discussed above but technically more involved due to extra terms (b) and (d) in Figure 12 and color averaging over the projectile proton wave function. Although bremsstrahlung terms from Figures 12(b) and 12(d) are formally of the leading twist due to interactions with distant spectator partons, numerically they are always tiny due to denominator suppression by large $\bar{Q}Q$ mass. Thus, the leading twist production terms from (b), (c), and (d) sets are relevant whereas the set (a) does not contain production terms and is a higher twist effect. Thus, like the case in diffractive Drell-Yan in the considered process the leading twist effect, at least, partly emerges due to intrinsic transverse motion of constituent quarks in the incoming proton. However, due to a non-Abelian nature

of this process extra leading twist terms production from the “production” mechanism, which are independent of the structure of the hadronic wave function, become important. Diffractive production cross sections of charm, beauty, and top quark pairs, $p + p \rightarrow \bar{Q}QX + p$, as functions of c.m.s. pp energy are shown in Figure 14. The experimental data points available from E690 [27] and CDF [28] experiments have been compared with theoretical predictions evaluated with corresponding phase space constraints (for more details, see [9]).

5.2. Single Diffractive Higgsstrahlung. Typically large Standard Model (SM) backgrounds and theoretical uncertainties due to higher order effects strongly limit the potential of inclusive Higgs boson production for spotting likely small but yet possible New Physics effects. Some of the SM extensions predict certain distortions in Higgs boson Yukawa couplings such that the precision multichannel measurements of the Higgs-heavy quarks couplings become a crucial test of the SM structure. As a very promising but challenging channel, the exclusive and diffractive Higgs production processes (involving rapidity gaps) offer new possibilities to constrain the backgrounds and open up more opportunities for New Physics searches (see, e.g., [64–71]).

The QCD-initiated gluon-gluon fusion $gg \rightarrow H$ mechanism via a heavy quark loop is one of the dominant and most studied Higgs bosons production modes in inclusive pp scattering which has led to its discovery at the LHC (for more information on Higgs physics highlights, see, e.g., [72–77] and references therein). The same mechanism is expected to provide an important Higgs production mode in single diffractive pp scattering as well as in central exclusive Higgs boson production [64, 65, 68]. The forward inclusive and diffractive Higgsstrahlung off intrinsic heavy flavor at $x_F \rightarrow 1$ has previously been studied in [78, 79], respectively.

Very recently, a new single diffractive production mode of the Higgs boson in association with a heavy quark pair $\bar{Q}Q$, namely, $pp \rightarrow X + \bar{Q}QH + p$, at large x_F where conventional factorization-based approaches are expected to fail has been studied in [20]. The latter process is an important background for diffractive Higgs boson hadroproduction off intrinsic heavy flavor. Here, we provide a short overview of this process which is analogical to forward diffractive $\bar{Q}Q$ production discussed above.

For a reasonably accurate estimate one retains only the dominant gluon-initiated leading twist terms illustrated in Figure 15 where the “active” gluon is coupled to the hard $\bar{Q}Q + H$ system, while the soft “screening” gluon couples to a spectator parton at a large impact distance. The latter is illustrated by tree-level diagrams with Higgs boson radiation off a heavy quark or Higgsstrahlung. In practice, however, one does not calculate the Feynman graphs explicitly in Figure 15. Instead one should adopt the generalized optical theorem within the Good-Walker approach to diffraction [3] such that a diffractive scattering amplitude turns out to be proportional to a difference between elastic scatterings of different Fock states [20]. The contributions where both “active” and “screening” gluons couple to partons at small

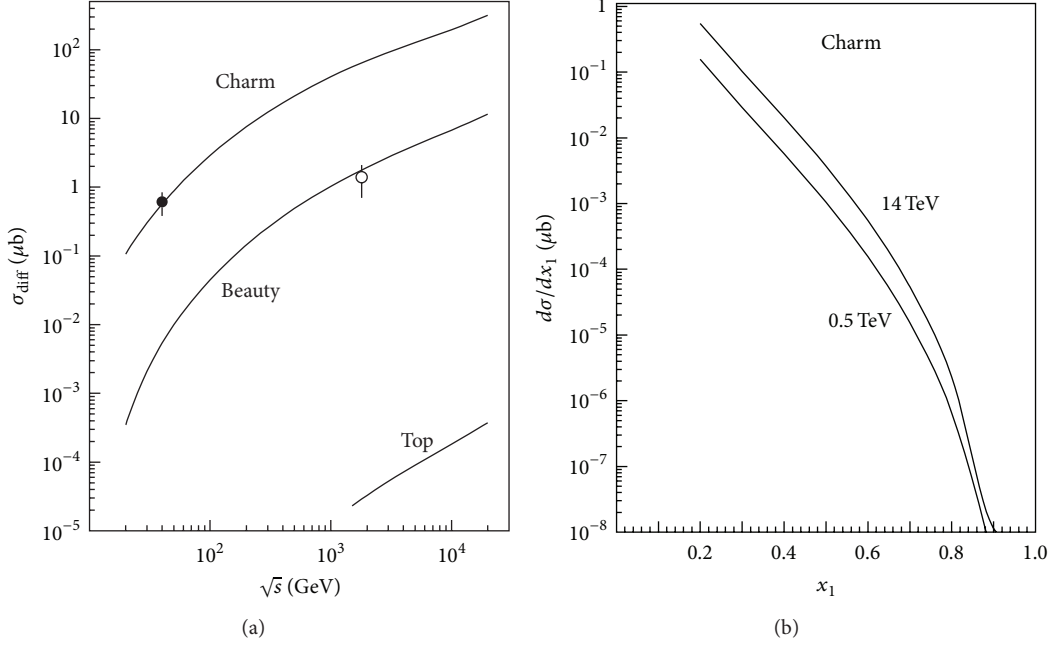


FIGURE 14: The total cross section of diffractive $c\bar{c}$, $b\bar{b}$, and $t\bar{t}$ pairs production as function of energy in comparison with experimental data from E690 [27] and CDF [28] experiments (a) and the differential cross section as function of fraction x_1 of the initial proton momentum carried by the charm quark (b) [9].

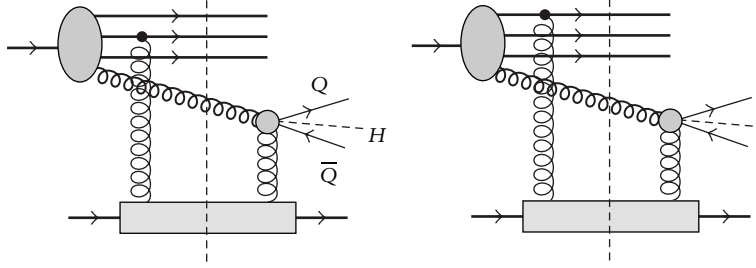


FIGURE 15: Dominant gluon-initiated contributions to the single diffractive $\bar{Q}Q + H$ production [20].

relative distances are the higher twist ones and thus are strongly suppressed by extra powers of the hard scale (see, e.g., [9]). This becomes obvious in the color dipole framework due to color transparency [11] making the medium more transparent for smaller dipoles.

The hard scales which control the diffractive Higgsstrahlung process are $\langle r^2 \rangle \sim 1/m_Q^2$ and $\langle \rho^2 \rangle \sim 1/\tau^2$, where $\tau^2 = M_H^2 + \alpha_3 M_{Q\bar{Q}}^2$ in terms of the Higgs boson mass, M_H , and the $Q\bar{Q}$ pair invariant mass, $M_{Q\bar{Q}}$. Another length scale here is the distance between i th and j th projectile partons, $\langle r_{ij}^2 \rangle \sim \langle R \rangle^2$, which is soft for light valence/sea quarks in the proton wave function. Before the hard gluon splits into $Q\bar{Q}H$ system it undergoes multiple splittings $g \rightarrow gg$ populating the projectile fragmentation domain with gluon radiation with momenta below the hard scale of the process $p_{\perp}^{\text{rad}} < M_{Q\bar{Q}H}$. The latter should be accounted for via a gluon PDF evolution.

The SD-to-inclusive ratio of the cross sections for different c.m. energies $\sqrt{s} = 0.5, 7, 14$ TeV and for two distinct

rapidities $Y = 0$ and 3 as functions of $\bar{Q}QH$ invariant mass M is shown in Figure 16(a). The ratio is similar to that for heavy quark production [9] and thus in good agreement with experimental data from the Tevatron. Note that this ratio has falling energy-dependence and rising M -dependence, where M is the invariant mass of the produced $\bar{Q}QH$ system. This is similar to what was found for diffractive Drell-Yan process [7, 8] and has the same origin, namely, breakdown of QCD factorization and the saturated form of the dipole cross section.

The differential cross sections of single diffractive $b\bar{b}$ and $t\bar{t}$ production in association with the Higgs boson are shown in Figure 16(b) as functions of x_1 variable at the LHC energy $\sqrt{s} = 14$ TeV implied that the Higgs boson transverse momentum is large; that is, $\kappa \geq m_H$. In this case the asymptotic dipole formula based upon the collinear projectile gluon PDF (32) and the first (quadratic) term in the dipole cross section is a good approximation and reproduces the exact k_{\perp} -factorization result for the inclusive Higgsstrahlung

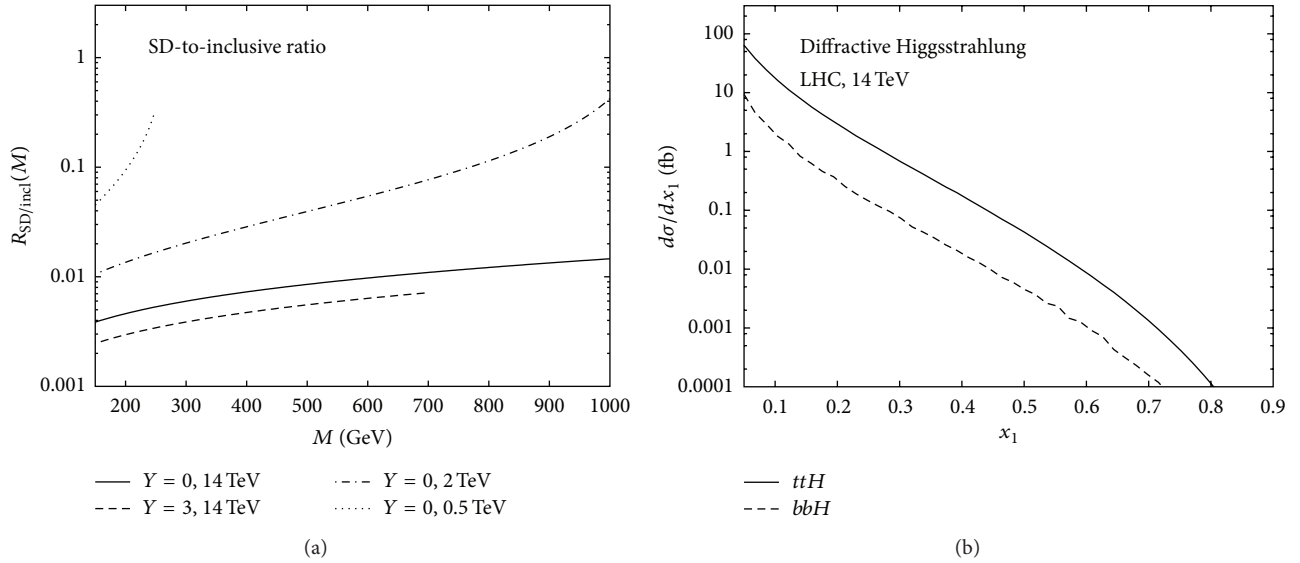


FIGURE 16: The SD-to-inclusive ratio $R(M)$ as a function of $\overline{Q}QH$ invariant mass M for different c.m. energies $\sqrt{s} = 0.5, 2, 14$ TeV (a) and the differential cross section $d\sigma/dx_1$ of the SD Higgsstrahlung off $t\bar{t}$ and $b\bar{b}$ pairs for $\sqrt{s} = 14$ TeV (b) [20].

transverse momentum distribution in both the shape and normalisation (for more details, see [20]). The contribution of diffractive gluon excitations to the Higgsstrahlung dominates the total Higgsstrahlung cross section due to a large yield from central rapidities. Besides, the SD Higgsstrahlung off top quarks is larger than that from the bottom while shapes of x_1 distributions are similar. Additional radiation of the Higgs boson enhances the contribution of heavy quarks and thus compensates the smallness of their diffractive production modes.

Analogically to other diffractive bremsstrahlung processes discussed in previous sections, breakdown of QCD factorization leads to a flatter hard scale dependence of the cross section. This is a result of leading twist behaviour which has been discussed above and which has been confirmed by the comparison of data on diffractive production of charm and beauty [9].

6. Summary

In this short review, we have discussed major properties and basic dynamics of single diffractive processes of γ^* , Z^0 , and W^\pm bosons production processes at the LHC, as well as leading twist heavy flavor hadroproduction at large Feynman x_F and diffractive Higgsstrahlung off heavy quarks. We outlined the manifestations of diffractive factorization breaking in these single diffractive reactions within the framework of color dipole description, which is suitable for studies of the interplay between soft and hard fluctuations. The latter reliably determine diffractive hadroproduction in the projectile fragmentation region.

The first, rather obvious source for violation of diffractive factorization, are related to the absorptive corrections (called

sometimes survival probability of large rapidity gaps). The absorptive corrections affect differently the diagonal and off-diagonal diffractive amplitudes [5, 51], leading to a breakdown of diffractive QCD factorization in hard diffractive processes, like diffractive radiation of heavy Abelian particles and heavy flavors. The dipole approach enables accounting for the absorptive corrections automatically at the amplitude level.

The second, more sophisticated reason for diffractive factorization breaking is specific for Abelian radiation; namely, a quark cannot radiate in the forward direction (zero-momentum transfer), where diffractive cross sections usually have a maximum. Forward diffraction becomes possible due to intrinsic transverse motion of quarks inside the proton, although the magnitude of the forward cross section remains very small [6, 7]. A much larger contribution to Abelian radiation in the forward direction in pp collisions comes from interaction with the spectator partons in the proton. Such an interplay of hard and soft dynamics is specific for the processes under consideration, which makes them different from diffractive DIS involving no comoving spectator partons.

These mechanisms of diffractive factorization breaking lead to rather unusual features of the leading twist diffractive Abelian radiation with respect to its hard scale and energy-dependence.

The outlined sources of factorization breaking are also presented in diffractive radiation of non-Abelian particles. Interactions of the radiated gluon make it possible to be radiated even at zero-momentum transfer. These processes have been quantitatively analysed in such important channels as diffractive heavy flavor production and Higgsstrahlung in the projectile fragmentation region. Further studies of these effects, both experimentally and theoretically, are of major importance for upcoming LHC measurements.

Conflict of Interests

The authors declare that there is no conflict of interests regarding the publication of this paper.

Acknowledgments


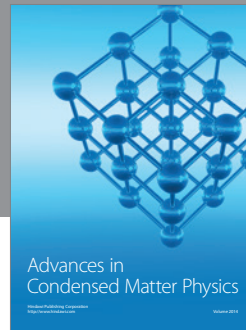
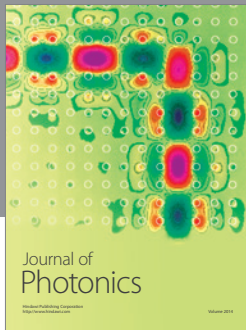
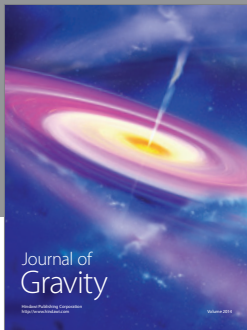
This study was partially supported by Fondecyt (Chile) Grants 1120920, 1130543, and 1130549 and by ECOS-Conicyt Grant no. C12E04. Roman Pasechnik was partially supported by Swedish Research Council Grant no. 2013-4287.

References

- [1] R. J. Glauber, "Cross sections in deuterium at high energies," *Physical Review*, vol. 100, no. 1, pp. 242–248, 1955.
- [2] E. Feinberg and I. Y. Pomeranchuk, *Il Nuovo Cimento*, supplement 3, p. 652, 1956.
- [3] M. L. Good and W. D. Walker, "Diffraction dissociation of beam particles," *Physical Review*, vol. 120, no. 5, pp. 1857–1860, 1960.
- [4] A. B. Kaidalov, "Diffractive production mechanisms," *Physics Reports*, vol. 50, no. 3, pp. 157–226, 1979.
- [5] B. Z. Kopeliovich, I. K. Potashnikova, and I. Schmidt, "Diffraction in QCD," *Brazilian Journal of Physics*, vol. 37, pp. 473–483, 2007.
- [6] B. Z. Kopeliovich, I. K. Potashnikova, I. Schmidt, and A. V. Tarasov, "Unusual features of Drell-Yan diffraction," *Physical Review D*, vol. 74, Article ID 114024, 2006.
- [7] R. S. Pasechnik and B. Z. Kopeliovich, "Drell-Yan diffraction: breakdown of QCD factorization," *The European Physical Journal C*, vol. 71, article 1827, 2011.
- [8] R. Pasechnik, B. Kopeliovich, and I. Potashnikova, "Diffractive gauge bosons production beyond QCD factorization," *Physical Review D*, vol. 86, Article ID 114039, 2012.
- [9] B. Z. Kopeliovich, I. K. Potashnikova, I. Schmidt, and A. V. Tarasov, "Diffractive excitation of heavy flavors: leading twist mechanisms," *Physical Review D*, vol. 76, Article ID 034019, 2007.
- [10] B. Z. Kopeliovich and B. Povh, "Interplay of soft and hard interactions in nuclear shadowing at high Q^2 and low x ," *Zeitschrift für Physik A Hadrons and Nuclei*, vol. 356, no. 4, pp. 467–470, 1997.
- [11] B. Z. Kopeliovich, L. I. Lapidus, and A. B. Zamolodchikov, "Dynamics of color in hadron diffraction on nuclei," *JETP Letters*, vol. 33, pp. 595–597, 1981.
- [12] G. Ingelman and P. E. Schlein, "Jet structure in high mass diffractive scattering," *Physics Letters B*, vol. 152, no. 3-4, pp. 256–260, 1985.
- [13] A. Brandt, "Evidence for a super-hard pomeron structure," *Physics Letters B*, vol. 297, no. 3-4, pp. 417–424, 1992.
- [14] R. Bonino, A. Brandt, J. Cheze et al., "Evidence for transverse jets in high-mass diffraction: UA8 experiment," *Physics Letters B*, vol. 211, no. 1-2, pp. 239–246, 1988.
- [15] F. Abe, H. Akimoto, A. Akopian et al., "Observation of diffractive W -boson production at the fermilab tevatron," *Physical Review Letters*, vol. 78, no. 14, pp. 2698–2703, 1997.
- [16] T. Aaltonen, B. Álvarez González, S. Amerio et al., "Diffractive W and Z production at the Fermilab Tevatron," *Physical Review D*, vol. 82, Article ID 112004, 2010.
- [17] K. A. Goulianos, "Factorization and scaling in hard diffraction," *AIP Conference Proceedings*, vol. 407, p. 527, 1997.
- [18] G. Kubasiak and A. Szczurek, "Inclusive and exclusive diffractive production of dilepton pairs in proton-proton collisions at high energies," *Physical Review D*, vol. 84, no. 1, Article ID 014005, 14 pages, 2011.
- [19] M. B. G. Ducati, M. M. Machado, and M. V. T. Machado, "Diffractive hadroproduction of W^\pm and Z^0 bosons at high energies," *Physical Review D*, vol. 75, Article ID 114013, 2007.
- [20] R. Pasechnik, B. Z. Kopeliovich, and I. K. Potashnikova, "Diffractive higgsstrahlung," <http://arxiv.org/abs/1403.2014>.
- [21] M. G. Ryskin, A. D. Martin, and V. A. Khoze, "Soft processes at the LHC, II: soft-hard factorisation breaking and gap survival," *The European Physical Journal C*, vol. 60, no. 2, pp. 265–272, 2009.
- [22] M. G. Ryskin, A. D. Martin, and V. A. Khoze, "High-energy strong interactions: from 'hard' to 'soft'," *The European Physical Journal C*, vol. 71, article 1617, 2011.
- [23] B. Z. Kopeliovich, A. Schäfer, and A. V. Tarasov, "Nonperturbative effects in gluon radiation and photoproduction of quark pairs," *Physical Review D*, vol. 62, Article ID 054022, 2000.
- [24] B. Z. Kopeliovich and L. I. Lapidus, "Quark—parton model for hadron—nucleus interactions," *Pisma v Zhurnal Eksperimentalnoi i Teoreticheskoi Fiziki*, vol. 28, p. 664, 1978.
- [25] H. I. Miettinen and J. Pumplin, "Diffraction scattering and the parton structure of hadrons," *Physical Review D*, vol. 18, no. 5, article 1696, 1978.
- [26] K. J. Golec-Biernat and M. Wusthoff, "Saturation effects in deep inelastic scattering at low Q^2 and its implications on diffraction," *Physical Review D*, vol. 59, Article ID 014017, 1998.
- [27] M. H. L. S. Wang, M. C. Berisso, D. C. Christian et al., "Diffractively produced charm final states in 800-GeV/c pp collisions," *Physical Review Letters*, vol. 87, Article ID 082002, 2001.
- [28] T. Affolder, H. Akimoto, A. Akopian et al., "Observation of diffractive b -quark production at the fermilab tevatron," *Physical Review Letters*, vol. 84, no. 2, pp. 232–237, 2000.
- [29] J. D. Bjorken, J. B. Kogut, and D. E. Soper, "Quantum electrodynamics at infinite momentum: scattering from an external field," *Physical Review D*, vol. 3, no. 6, pp. 1382–1399, 1971.
- [30] J. Bartels, K. J. Golec-Biernat, and H. Kowalski, "Modification of the saturation model: Dokshitzer-Gribov-Lipatov-Altarelli-Parisi evolution," *Physical Review D*, vol. 66, no. 1, Article ID 014001, 9 pages, 2002.
- [31] R. M. Barnett, C. D. Carone, D. E. Groom et al., "Particle physics summary: a digest of the 1996 review of particle physics," *Reviews of Modern Physics*, vol. 68, pp. 611–732, 1996.
- [32] S. R. Amendolia, M. Arik, B. Badelek et al., "A measurement of the space-like pion electromagnetic form factor," *Nuclear Physics B*, vol. 277, pp. 168–196, 1986.
- [33] B. Z. Kopeliovich, H. J. Pirner, A. H. Rezaeian, and I. Schmidt, "Azimuthal anisotropy of direct photons," *Physical Review D*, vol. 77, no. 3, Article ID 034011, 6 pages, 2008.
- [34] B. Z. Kopeliovich, I. K. Potashnikova, I. Schmidt, and J. Soffer, "Damping of forward neutrons in pp collisions," *Physical Review D*, vol. 78, Article ID 014031, 2008.
- [35] B. Z. Kopeliovich, A. H. Rezaeian, and I. Schmidt, "Azimuthal Asymmetry of pions in pp and pA collisions," *Physical Review D*, vol. 78, no. 11, Article ID 114009, 15 pages, 2008.
- [36] B. Z. Kopeliovich, J. Raufeisen, and A. V. Tarasov, "The color dipole picture of the Drell-Yan process," *Physics Letters B*, vol. 503, no. 1-2, pp. 91–98, 2001.

- [37] A. Donnachie and P. V. Landshoff, “Hard diffraction: production of high p_T jets, W or Z, and Drell-Yan pairs,” *Nuclear Physics B*, vol. 303, pp. 634–652, 1988.
- [38] J. C. Collins, D. E. Soper, and G. F. Sterman, “Factorization of hard processes in QCD,” *Advanced Series on Directions in High Energy Physics*, vol. 5, pp. 1–91, 1989.
- [39] A. Donnachie and P. V. Landshoff, “Hard diffraction: production of high p_T jets, W or Z, and Drell-Yan pairs,” *Nuclear Physics B*, vol. 303, no. 4, pp. 634–652, 1988.
- [40] G. Bertsch, S. J. Brodsky, A. S. Goldhaber, and J. G. Gunion, “Diffractive excitation in quantum chromodynamics,” *Physical Review Letters*, vol. 47, no. 5, pp. 297–300, 1981.
- [41] B. Z. Kopeliovich, “Soft component of hard reactions and nuclear shadowing (DIS, Drell-Yan reaction, heavy quark production),” in *Proceedings of the Workshop Hirscheegg 95: Dynamical Properties of Hadrons in Nuclear Matter*, H. Feldmeier and W. Nörenberg, Eds., p. 102, Darmstadt, Germany, 1995, <http://arxiv.org/abs/hep-ph/9609385>.
- [42] S. J. Brodsky, A. Hebecker, and E. Quack, “Drell-Yan process and factorization in impact parameter space,” *Physical Review D*, vol. 55, no. 5, pp. 2584–2590, 1997.
- [43] B. Z. Kopeliovich, A. Schäfer, and A. V. Tarasov, “Bremsstrahlung of a quark propagating through a nucleus,” *Physical Review C*, vol. 59, no. 3, pp. 1609–1619, 1999.
- [44] J. Raufeisen, J.-C. Peng, and G. C. Nayak, “Parton model versus color dipole formulation of the Drell-Yan process,” *Physical Review D*, vol. 66, Article ID 034024, 2002.
- [45] S. J. Brodsky and P. Hoyer, “A bound on the energy loss of partons in nuclei,” *Physics Letters B*, vol. 298, pp. 165–170, 1993.
- [46] L. D. Landau and I. Y. Pomeranchuk, “Limits of applicability of the theory of bremsstrahlung electrons and pair production at high-energies,” *Zhurnal Eksperimentalnoi i Teoreticheskoi Fiziki*, vol. 92, pp. 535–536, 1953 (Russian).
- [47] J. C. Collins, L. Frankfurt, and M. Strikman, “Diffractive hard scattering with a coherent pomeron,” *Physics Letters B*, vol. 307, no. 1-2, pp. 161–168, 1993.
- [48] J. C. Collins, “Proof of factorization for diffractive hard scattering,” *Physical Review D*, vol. 57, no. 5, pp. 3051–3056, 1998.
- [49] B. Z. Kopeliovich, I. K. Potashnikova, B. Povh, and E. Predazzi, “Nonperturbative gluon radiation and energy dependence of elastic scattering,” *Physical Review Letters*, vol. 85, no. 3, pp. 507–510, 2000.
- [50] B. Z. Kopeliovich, I. K. Potashnikova, B. Povh, and E. Predazzi, “Soft QCD dynamics of elastic scattering in the impact parameter representation,” *Physical Review D*, vol. 63, no. 5, Article ID 054001, 2001.
- [51] B. Z. Kopeliovich, I. K. Potashnikova, I. Schmidt, and M. Siddikov, “Breakdown of partial conservation of axial current in diffractive neutrino interactions,” *Physical Review C*, vol. 84, Article ID 024608, 2011.
- [52] T. Schäfer and E. V. Shuryak, “Instantons in QCD,” *Reviews of Modern Physics*, vol. 70, article 323, 1998.
- [53] E. V. Shuryak and I. Zahed, “Understanding nonperturbative deep-inelastic scattering: instanton-induced inelastic dipole-dipole cross section,” *Physical Review D*, vol. 69, Article ID 014011, 2004.
- [54] B. Z. Kopeliovich, I. K. Potashnikova, B. Povh, and I. Schmidt, “Evidences for two scales in hadrons,” *Physical Review D*, vol. 76, Article ID 094020, 2007.
- [55] A. H. Mueller and B. Patel, “Single and double BFKL pomeron exchange and a dipole picture of high energy hard processes,” *Nuclear Physics B*, vol. 425, no. 3, pp. 471–488, 1994.
- [56] N. N. Nikolaev and B. G. Zakharov, “The pomeron in diffractive deep inelastic scattering,” *Journal of Experimental and Theoretical Physics*, vol. 78, no. 5, article 598, 1994.
- [57] B. Z. Kopeliovich, I. K. Potashnikova, B. Povh, and I. Schmidt, “Pion structure function at small x from deep-inelastic scattering data,” *Physical Review D*, vol. 85, Article ID 114025, 2012.
- [58] S. Chekanov, M. Derrick, S. Magill et al., “Exclusive ρ^0 production in deep inelastic scattering at HERA,” *PMC Physics A*, vol. 1, article 6, 2007.
- [59] J. Bartels, S. Bondarenko, K. Kutak, and L. Motyka, “Exclusive Higgs boson production at the CERN LHC: hard rescattering corrections,” *Physical Review D*, vol. 73, Article ID 093004, 2006.
- [60] K. Wijesooriya, P. E. Reimer, and R. J. Holt, “Pion parton distribution function in the valence region,” *Physical Review C*, vol. 72, no. 6, Article ID 065203, 5 pages, 2005.
- [61] B. Z. Kopeliovich, J. Nemchik, I. K. Potashnikova, M. B. Johnson, and I. Schmidt, “Breakdown of QCD factorization at large Feynman x ,” *Physical Review C*, vol. 72, Article ID 054606, 2005.
- [62] B. Z. Kopeliovich and A. V. Tarasov, “Gluon shadowing in heavy flavor production off nuclei,” *Nuclear Physics A*, vol. 710, no. 1-2, pp. 180–217, 2002.
- [63] J. F. Gunion and G. Bertsch, “Hadronization by color bremsstrahlung,” *Physical Review D*, vol. 25, no. 3, pp. 746–753, 1982.
- [64] V. A. Khoze, A. D. Martin, and M. G. Ryskin, “The rapidity gap Higgs signal at LHC,” *Physics Letters B*, vol. 401, no. 3-4, pp. 330–336, 1997.
- [65] V. A. Khoze, A. D. Martin, and M. G. Ryskin, “Can the Higgs be seen in rapidity gap events at the Tevatron or the LHC?” *The European Physical Journal C*, vol. 14, no. 3, pp. 525–534, 2000.
- [66] V. A. Khoze, A. D. Martin, and M. G. Ryskin, “Double-diffractive processes in high-resolution missing-mass experiments at the Tevatron,” *The European Physical Journal C*, vol. 19, no. 3, pp. 477–483, 2001, Erratum in: *The European Physical Journal C*, vol. 20, p. 599, 2001.
- [67] V. A. Khoze, A. D. Martin, and M. G. Ryskin, “Prospects for new physics observations in diffractive processes at the LHC and Tevatron,” *The European Physical Journal C*, vol. 23, no. 2, pp. 311–327, 2002.
- [68] A. B. Kaidalov, V. A. Khoze, A. D. Martin, and M. G. Ryskin, “Extending the study of the Higgs sector at the LHC by proton tagging,” *European Physical Journal C*, vol. 33, no. 2, pp. 261–271, 2004.
- [69] S. Heinemeyer, V. A. Khoze, M. G. Ryskin, W. J. Stirling, M. Tasevsky, and G. Weiglein, “Studying the MSSM Higgs sector by forward proton tagging at the LHC,” *European Physical Journal C*, vol. 53, no. 2, pp. 231–256, 2008.
- [70] S. Heinemeyer, V. A. Khoze, M. G. Ryskin, M. Tasevsky, and G. Weiglein, “BSM Higgs physics in the exclusive forward proton mode at the LHC,” *The European Physical Journal C*, vol. 71, article 1649, 2011.
- [71] M. Tasevsky, “Exclusive MSSM Higgs production at the LHC after run I,” *The European Physical Journal C*, vol. 73, article 2672, 2013.
- [72] G. Aad, T. Abajyan, B. Abbott et al., “Observation of a new particle in the search for the Standard Model Higgs boson with the ATLAS detector at the LHC,” *Physics Letters B*, vol. 716, no. 1, pp. 1–29, 2012.
- [73] S. Chatrchyan, V. Khachatryan, A. M. Sirunyan et al., “Observation of a new boson at a mass of 125 GeV with the CMS

- experiment at the LHC,” *Physics Letters B*, vol. 716, no. 1, pp. 30–61, 2012.
- [74] M. S. Carena and H. E. Haber, “Higgs Boson theory and phenomenology,” *Progress in Particle and Nuclear Physics*, vol. 50, no. 1, pp. 63–152, 2003.
- [75] S. Dittmaier, C. Mariotti, G. Passarino et al., *Handbook of LHC Higgs Cross Sections: 1. Inclusive Observables*, CERN, Geneva, Switzerland, 2011.
- [76] S. Dittmaier, C. Mariotti, G. Passarino et al., *Handbook of LHC Higgs Cross Sections: 2. Differential Distributions*, European Organization for Nuclear Research (CERN), Geneva, Switzerland, 2012.
- [77] S. Heinemeyer, C. Mariotti, G. Passarino et al., *Handbook of LHC Higgs Cross Sections: 3. Higgs Properties*, CERN, Geneva, Switzerland, 2013.
- [78] S. J. Brodsky, A. S. Goldhaber, B. Z. Kopeliovich, and I. Schmidt, “Higgs hadroproduction at large Feynman x ,” *Nuclear Physics B*, vol. 807, no. 1-2, pp. 334–347, 2009.
- [79] S. J. Brodsky, B. Kopeliovich, I. Schmidt, and J. Soffer, “Diffractive Higgs production from intrinsic heavy flavors in the proton,” *Physical Review D*, vol. 73, no. 11, Article ID 113005, 2006.



Hindawi

Submit your manuscripts at
<http://www.hindawi.com>

